International Journal of Bifurcation and Chaos, Vol. 27, No. 3 (2017) 1750043 (28 pages)

DOI: 10.1142/S0218127417500432

Multistable Phenomena Involving Equilibria and Periodic Motions in Predator–Prey Systems

Jiao Jiang
Department of Mathematics, Shanghai Maritime University, Shanghai 201306, P. R. China
jiaojiang@shmtu.edu.cn

Pei Yu*
Department of Applied Mathematics, Western University, London, Ontario, N6A 5B7, Canada
pyu@uwo.ca

Received December 22, 2016

In this paper, we consider a number of predator–prey systems with various types of functional responses. Detailed analysis on the dynamics and bifurcations of the systems are given. Particular attention is focused on the complex dynamics due to bifurcation of limit cycles, which may generate bistable or tristable phenomena involving equilibria and oscillating motions. It is shown that predator–prey systems can exhibit such bistable or tristable phenomena due to Hopf bifurcation, giving rise to the coexistence of stable equilibria and stable periodic solutions. Explicit conditions on the system parameters are derived which can be used to determine the number of Hopf bifurcations, the stability of bifurcating limit cycles, and the parameter regime where the bistable or tristable phenomenon occurs. The method developed in this paper can be applied to study certain interesting patterns of complex dynamical behaviors in biological or other physical systems.

Keywords: Predator–prey system; Holling type functional response; Hopf bifurcation; bistable; tristable; limit cycle; normal form; focus value.

1. Introduction

The predator–prey model is an application of the nonlinear differential systems in mathematical biology/ecology to model the predator–prey relationship of a simple population system. The earliest predator–prey model is the Lotka–Volterra equations [Lotka, 1920; Volterra, 1926], describing the population change of two species, one as predator and the other as prey. The model is given in the form of differential equations as

$$\begin{aligned} \dot{x} &= ax - bxy, \\ \dot{y} &= cxy - dy, \end{aligned} \tag{1}$$

where dot denotes differentiation with respect to time t, x and y represent the densities of the prey and the predator, respectively; and a, b, c and d are positive parameters describing the interaction of the two species. It is easy to show that system (1) is integrable and its solutions can be obtained by using an integrating factor $\frac{1}{xy}$ as

$$V(x, y) = -cx - by + d \ln x + a \ln y$$

and $V(x, y) = C$ (C is an arbitrary constant), called first integral, describes closed orbits (level curves) in the x–y place, implying that all solutions of system (1) are periodic. Note that these

*Author for correspondence

closed orbits are not isolated and are thus not limit cycles.

Later, the model was extended to include density dependence prey growth and function responses called Holling type forms [Holling, 1959a, 1959b], and the model became known as the Rosenzweig–MacArthur model [Rosenzweig & MacArthur, 1963]. In 1989 Arditi and Ginzburg [1989] further developed an alternative to the Lotka–Volterra predator–prey model (and its common prey dependent generalizations) by introducing the ratio dependent function into the model, known today as Arditi–Ginzburg model. Now, the predator–prey model and its generalizations are used to consider not only population problems, but also other phenomena, depending on the specific setting of applications, such as those in modeling plant-herbivore, parasite-host, tumor cells-immune system, susceptible-infectious, etc.

A latest and more sophisticated classification of predator–prey models is based on the so-called Gause type predator–prey model, which takes the following general form [Freedman, 1980],

$$\dot{x} = xg(x,K) - yp(x), \quad \dot{y} = y[-d + dq(x)], \qquad (2)$$

where $g(x,K)$ is a continuous and differentiable function describing the specific growth rate of the prey in the absence of predators. The logistic growth $g(x,K) = r(1-\frac{x}{K})$ is usually considered as a prototype, satisfying $g(0,K) = r > 0$, $g(K,K) = 0$, $g_x(K,K) < 0$, $g_x(x,K) \le 0$, and $g_K(x,K) > 0$ for any $x > 0$.

The functional response $p(x)$ of predators to the prey, which is continuous and differentiable, satisfying $p(0) = 0$, describes the change in the density of the prey attacked per unit time per predator as the prey density changes. It should be noted that in general, $p(x)$ depends upon many factors such as variation of the prey density, the efficiency with which predators can search out and kill the prey, the handling time, etc. The following functional response functions have been extensively used in modeling population dynamics.

(i) Lotka–Volterra type: $p(x) = mx$, where m is a positive constant, which is an unbounded function.

(ii) Holling type II: $p(x) = \frac{mx}{a+x}$, where m and a are positive constants, and a is called the half-saturation constant, which is bounded, satisfying $p'(x) > 0$ and $\lim_{x\to\infty} p(x) = m$.

(iii) Generalized Holling type III or sigmoidal: $p(x) = \frac{mx^2}{ax^2+bx+1}$, where m and a are positive constants and b is a constant. When $b = 0$, it is called the Holling type III response function. When $b > -2\sqrt{a}$ (so that $ax^2 + bx + 1 > 0$ and hence $p(x) > 0$), it is called the generalized Holling type III or sigmoidal functional response [Bazykin, 1998].

The function $q(x)$ in system (2) describes how predator converts the consumed prey into the growth of predators and the parameter c indicates the efficiency of predators in converting consumed prey into their growth, while d is the predator mortality rate. In the past studies, $q(x)$ takes three typical forms:

(A) $q(x) = p(x)$ which is used in the most classical predator–prey models.

(B) $q(\frac{x}{y}) = p(\frac{x}{y})$, which is not dependent on the prey density, but instead on the ratio of the prey to predators.

(C) $q(\frac{y}{x})$ depending on the ratio of the predators to their prey, and the typical second equation of (2) is given by $\dot{y} = yq(\frac{y}{x}) = sy(1-\frac{y}{hx})$ while the first equation of (2) still takes $p(x)$.

Thus, combining these three types of function $q(x)$ with the three types of function $p(x)$, we obtain nine systems:

$$\mathrm{A_i}: \begin{cases} \dot{x} = rx\Big(1-\dfrac{x}{K}\Big) - mxy, \\ \dot{y} = y(mcx - d); \end{cases} \qquad (3)$$

$$\mathrm{A_{ii}}: \begin{cases} \dot{x} = rx\Big(1-\dfrac{x}{K}\Big) - \dfrac{mxy}{a+x}, \\ \dot{y} = y\Big(\dfrac{mcx}{a+x} - d\Big); \end{cases} \qquad (4)$$

$$\mathrm{A_{iii}}: \begin{cases} \dot{x} = rx\Big(1-\dfrac{x}{K}\Big) - \dfrac{mx^2y}{ax^2+bx+1}, \\ \dot{y} = y\Big(\dfrac{mcx^2}{ax^2+bx+1} - d\Big); \end{cases} \qquad (5)$$

$$\mathrm{B_i}: \begin{cases} \dot{x} = rx\Big(1-\dfrac{x}{K}\Big) - mx, \\ \dot{y} = mcx - dy; \end{cases} \qquad (6)$$

$$\mathrm{B_{ii}}: \begin{cases} \dot{x} = rx\Big(1 - \dfrac{x}{K}\Big) - \dfrac{mxy}{x + ay}, \\ \dot{y} = y\Big(\dfrac{mcx}{x + ay} - d\Big); \end{cases} \tag{7}$$

$$\mathrm{B_{iii}}: \begin{cases} \dot{x} = rx\Big(1 - \dfrac{x}{K}\Big) - \dfrac{mx^2y}{ax^2 + bxy + y^2}, \\ \dot{y} = y\Big(\dfrac{mcx^2}{ax^2 + bxy + y^2} - d\Big); \end{cases} \tag{8}$$

$$\mathrm{C_i}: \begin{cases} \dot{x} = rx\Big(1 - \dfrac{x}{K}\Big) - mxy, \\ \dot{y} = sy\Big(1 - \dfrac{y}{hx}\Big); \end{cases} \tag{9}$$

$$\mathrm{C_{ii}}: \begin{cases} \dot{x} = rx\Big(1 - \dfrac{x}{K}\Big) - \dfrac{mxy}{a + x}, \\ \dot{y} = sy\Big(1 - \dfrac{y}{hx}\Big), \end{cases} \tag{10}$$

$$\mathrm{C_{iii}}: \begin{cases} \dot{x} = rx\Big(1 - \dfrac{x}{K}\Big) - \dfrac{mx^2y}{ax^2 + bx + 1}, \\ \dot{y} = sy\Big(1 - \dfrac{y}{hx}\Big). \end{cases} \tag{11}$$

Note that all the parameters should take positive values, except for b which may also take zero or negative values, provided $b > -2\sqrt{a}$.

If in the second equation of the above systems, we add a negative, constant term, which measures the rate of *harvesting* or *removal* [Xiao *et al.*, 2006], we are able to analyze the general effect of harvesting on these models. We leave the investigation on these models as future work.

A common natural and important phenomenon which usually appears in predator–prey models is self-sustained oscillations, giving rise to limit cycles. Such special periodic solutions describes a dynamical balance between predator and prey — a more realistic situation. Thus, identifying the existence of limit cycles and determining their stability become very important in analyzing the dynamics of such models. Moreover, it has been found that studying bifurcation of multiple limit cycles and determining the number of limit cycles even play a more significant role in applications since it may cause bistable or even tristable phenomena which involve not only stable equilibria but also stable motions [Ruan & Wang, 2003; Wang *et al.*, 2013; Zhang *et al.*, 2013, 2014a, 2014b; Yu & Lin, 2016]. However, it has also been shown in these publications that even for two-dimensional predator–prey models or epidemic models, determining whether the system can have more than one limit cycle bifurcating from a Hopf critical point is not easy. For example, in the studies of most disease models, researchers often merely investigate bistable states which involve only equilibrium solutions due to difficulty of identifying multiple limit cycles. Nevertheless, stable disease-free equilibrium and periodic disease motion may often coexist in real situations. In such a more realistic case, it is necessary to consider bifurcation of limit cycles and determine their stability. Very recently, we have found bifurcation of two limit cycles in the vicinity of a stable equilibrium in an HIV model [Yu *et al.*, 2016; Yu & Lin, 2016] due to Hopf bifurcation, showing the interesting bistable or even tristable phenomenon. We derived explicit conditions on the system parameters and used them to determine the number of bifurcating limit cycles and their stability. It should be mentioned that in recent years numerical bifurcation methods and computer software have been developed and widely applied to study bifurcations of dynamical systems (e.g. see [Meijer *et al.*, 2013]). This is a quite a powerful tool in applications since it can generate a bifurcation diagram in the parameter space, giving a global picture to help analysis. However, its drawback is that it cannot provide closed formulae for an analytic study. In particular, it is very difficult or impossible to use this tool to identify bifurcation of multiple limit cycles around an isolated singularity. In such cases, analytic and explicit formulas are necessary to be obtained.

The main aim of this paper is to investigate bifurcation of limit cycles which may occur in systems (3)–(7) due to Hopf bifurcation, and leave systems (8)–(11) to be studied in forthcoming papers. In particular, for each model to be considered in the whole parameter space, we will show the positivity and boundedness of solutions, find the equilibrium solutions and determine their stability, identify the Hopf bifurcation points and derive explicit conditions to determine the regime in the parameter space where the system can exhibit bistable or tristable phenomenon. It should be pointed out that even for two-dimensional dynamical systems, Hopf bifurcation is not the only source to general bifurcation of limit cycles. Homoclinic orbits may

occur in such systems due to Bogdanov–Takens bifurcation, which is characterized by a double-zero eigenvalue at a critical point, and limit cycles can bifurcate near homoclinic orbits. For the models (3)–(7) considered in this paper, we will show that only model (5) can exhibit Bogdanov–Takens bifurcation. However, we will mainly focus on Hopf and generalized Hopf bifurcations in this paper, and leave the Bogdanov–Takens bifurcation as future work.

The rest of the paper is organized as follows. In the next section, we will present a method for computing normal forms used in the following sections to study bifurcation of limit cycles due to Hopf bifurcation. In Sec. 3, we give detailed studies on the five models (3)–(7) one by one to analyze bifurcations and determine existence of limit cycles. The main effort is devoted to study Hopf and generalized Hopf bifurcations for Model A_{iii} [see Eq. (5)]. Simulations are given in Sec. 4 to demonstrate the analytical predictions. Finally, the conclusion is drawn in Sec. 5.

2. Methodology

The basic idea of the methodology applied in this paper is described in this section. Roughly speaking, for a given nonlinear dynamical system associated with a Hopf bifurcation, we want to find the simple quantities which can be used to determine the number of limit cycles bifurcating from a Hopf critical point and their stability. These quantities are usually called focus values (or Lyapunov constants), which can be obtained via computing the normal forms of general n-dimensional nonlinear systems.

Consider the following general n-dimensional differential system:

$$\dot{\mathbf{z}} = A\mathbf{z} + \mathbf{f}(\mathbf{z}), \quad \mathbf{z} \in \mathbf{R}^n, \quad \mathbf{f} : \mathbf{R}^n \to \mathbf{R}^n, \tag{12}$$

where $A\mathbf{z}$ and $\mathbf{f}(\mathbf{z})$ represent the linear and nonlinear parts of the system, respectively. Suppose that $\mathbf{f}(\mathbf{0}) = D\mathbf{f}(\mathbf{0}) = \mathbf{0}$, implying that $\mathbf{z} = 0$ is a fixed point of the system. Also, it is assumed that $\mathbf{f}(\mathbf{z})$ is analytic and can be expanded into Taylor series in $\mathbf{z}$. In general, matrix A may contain eigenvalues with negative, positive and zero real parts, and thus system (12) may consist of stable, unstable and center manifolds. However, in real applications, a system with unstable manifold is usually unstable and the first task will be stabilizing the system. Therefore, without loss of generality, we assume that system (12) only contains stable and center manifolds.

In normal form computation, the first step is usually to introduce a linear transformation into (12) such that its linear part becomes the Jordan canonical form. Note that for a linear system, the Jordan canonical form is the normal form of the system. Thus, introducing a linear transformation $\mathbf{z} = T\mathbf{x}$ into system (12) yields

$$\dot{\mathbf{x}} = J\mathbf{x} + \mathbf{f}(\mathbf{x}), \quad \mathbf{x} \in \mathbf{R}^n, \quad \mathbf{f} : \mathbf{R}^n \to \mathbf{R}^n, \tag{13}$$

where $J = \mathrm{diag}(J_1, J_2)$, and both J_1 and J_2 are in Jordan canonical forms, with $\mathrm{Re}(\lambda(J_1)) = 0$ and $\mathrm{Re}(\lambda(J_2)) < 0$.

Based on system (13), by applying the center manifold theory (e.g. see [Carr, 1981]) and normal form theory (e.g. see [Guckenheimer & Holmes, 1993; Chow *et al.*, 1994; Kuznetsov, 1998; Gazor & Yu, 2012]), as well as the computation methods using computer algebra systems (e.g. see [Yu, 1998; Yu & Leung, 2003; Tian & Yu, 2013, 2014; Han & Yu, 2012]), we obtain the normal form expressed in polar coordinates:

$$\begin{aligned} \dot{r} &= r(v_0 + v_1 r^2 + v_2 r^4 + \cdots + v_k r^{2k} + \cdots), \\ \dot{\theta} &= \omega_c + \tau_0 + \tau_1 r^2 + \tau_2 r^4 + \cdots + \tau_k r^{2k} + \cdots, \end{aligned} \tag{14}$$

where r and θ represent the amplitude and phase of motion, respectively. v_k $(k = 0, 1, 2, \ldots)$ is called the kth-order focus value. v_0 and τ_0 are obtained from linear analysis. The first equation of (14) can be used for studying bifurcation and stability of limit cycles, while the second equation can be used to determine the frequency of the bifurcating periodic motion. Moreover, the coefficients τ_j can be used to determine the order or critical periods of a center (when $v_j = 0$, $j \geq 0$).

The Maple programs developed in [Yu, 1998; Tian & Yu, 2013, 2014] for computing the normal form of Hopf bifurcation have been cross-verified for many mathematical and practical systems. The normal forms obtained by using the different programs are either identical or different by only a positive constant factor.

Once the focus values (or the Lyapunov constants) for a given system are obtained, we want to use these quantities to determine the bifurcation of limit cycles. The basic idea of finding k small-amplitude limit cycles in system (12) associated with a Hopf bifurcation around the origin is as follows: First, find the conditions based on the original system coefficients such that $v_0 = v_1 = \cdots = v_{k-1} = 0$ (note that $v_0 = 0$ is automatically satisfied

at the critical point), but $v_k \neq 0$, and then perform appropriate small perturbations to prove the existence of k limit cycles. This indicates that the procedure for finding multiple limit cycles involves two steps: Computing the focus values (i.e. computing the normal form) or the Lyapunov constants, and solving multivariate coupled nonlinear polynomial equations: $v_0 = v_1 = \cdots = v_{k-1} = 0$. In the following, we give sufficient conditions for the existence of k small-amplitude limit cycles. (The proof can be found in [Yu & Han, 2005].)

Lemma 1. *Suppose that the focus values depend on k parameters, ε_j $(j = 1, 2, \ldots, k)$, expressed as*

$$v_j = v_j(\varepsilon_1, \varepsilon_2, \ldots, \varepsilon_k), \quad j = 0, 1, \ldots, k, \quad (15)$$

satisfying

$$\begin{aligned} &v_j(\varepsilon_{1c}, \ldots, \varepsilon_{kc}) = 0, \quad j = 0, 1, \ldots, k-1, \\ &v_k(\varepsilon_{1c}, \ldots, \varepsilon_{kc}) \neq 0, \quad \textit{and} \\ &\operatorname{rank}\left[\frac{\partial(v_0, v_1, \ldots, v_{k-1})}{\partial(\varepsilon_1, \varepsilon_2, \ldots, \varepsilon_k)}(\varepsilon_{1c}, \ldots, \varepsilon_{kc})\right] = k. \end{aligned} \quad (16)$$

Then, for any given $\varepsilon_0 > 0$, there exist $\varepsilon_1, \varepsilon_2, \ldots, \varepsilon_k$ and $\delta > 0$ with $|\varepsilon_j - \varepsilon_{jc}| < \varepsilon_0$, $j = 1, 2, \ldots, k$ such that the equation, $\sum_{j=0}^{k} v_j r^{2j} = 0$, has exactly k real positive roots for r, i.e. system (12) has exactly k limit cycles, in a δ-ball with the center at the origin.

To demonstrate the use of the above theorem, we take Bautin's system as an example to show the computation of focus values and perturbations to obtain three small-amplitude limit cycles (e.g. see [Yu & Corless, 2009]). The quadratic Bautin's system can be written in the form of [Bautin, 1952]

$$\begin{aligned} \dot{x} &= ax + y + x^2 + (b + 2d)xy + cy^2 \\ \dot{y} &= -x + ay + dx^2 + (e - 2)xy - dy^2, \end{aligned} \quad (17)$$

where a, b, c, d and e are real parameters. It is clear that $v_0 = a$. To compute higher-order focus values, setting $v_0 = a = 0$, we obtain $v_1 = -\frac{1}{8}(c + 1)b$. Then, setting $v_1 = 0$, one may take either $b = 0$ or $c = -1$. However, it can be shown that $c = -1$ yields a center at the origin. So, choosing $b = 0$ results in $v_2 = -\frac{1}{48}de(c + 1)(5c - e + 5)$, which indicates that one must choose $e = 5(c + 1)$ to obtain $v_2 = 0$, under which $v_3 = -\frac{25}{64}d(c + 1)^3(c + 2c^2 + d^2)$. If we set $v_3 = 0$, then $v_4 = 0$ too. Actually, Bautin showed that setting v_3 to be zero leads to a center. Therefore, one can only choose three parameters such that $v_0 = v_1 = v_2 = 0$, but $v_3 \neq 0$, implying that at most three small-amplitude limit cycles exist around the origin.

To prove the existence of three small-amplitude limit cycles, we apply appropriate perturbations such that the perturbed focus values satisfy the sufficient conditions given in Lemma 1. There are infinitely many choices for the parameter values. Note that due to a scaling applied to system (17), the focus values for the original system can be adjusted to any small values using a free parameter in the original system. Under the critical conditions:

$$a = 0, \quad b = 0, \quad e = 5(c + 1),$$

we have $v_0 = v_1 = v_2 = 0$, $v_3 = -\frac{25}{64}d(c + 1)^3(c + 2c^2 + d^2)$. Since exactly one parameter is used for each of the three focus values, v_0, v_1 and v_2, the perturbations for the quadratic system is straightforward, as shown below.

For convenience, suppose $d(c + 1)(c + 2c^2 + d^2) > 0$, and thus $v_3 < 0$. Further, for definiteness, we may assume that $d > 0$ and $c > 0$, since we are not interested in finding all solutions (which we are certainly able to obtain) but only in the existence of the three small-amplitude limit cycles. Then, we want to give a perturbation to $e = 5(c + 1)$ such that $v_2 > 0$ and $0 < v_2 \ll -v_3$. We can find the derivative of v_2 with respect to e, evaluated at the critical values as $\frac{dv_2}{de} = \frac{5}{48}d(c + 1)^2 > 0$. So we may select $\varepsilon_1 > 0$ such that $e = 5(c + 1) + \varepsilon_1$. Then the perturbed v_2 is

$$\begin{aligned} v_2 &= \frac{d}{48}[5(c + 1)^2\varepsilon_1 + (c + 1)\varepsilon_1^2] \\ &\approx \frac{5}{48}d(c + 1)^2\varepsilon_1 > 0 \end{aligned}$$

and thus $0 < v_2 \ll -v_3$ as long as $0 < \varepsilon_1 \ll 1$.

Next, we want to perturb v_1 such that the perturbed values satisfy $0 < -v_1 \ll v_2 \ll -v_3$. Similarly, we find $\frac{dv_1}{db} = -\frac{1}{8}(c+1) < 0$, implying that we should perturb b from $b = 0$ to $b = 0 + \varepsilon_2$. Thus, the perturbed value of v_1 is given by $v_1 = -\frac{1}{8}(c+1)\varepsilon_2$, where $0 < \varepsilon_2 \ll \varepsilon_1 \ll 1$ which guarantees that $0 < -v_1 \ll v_2$.

Finally, we need a perturbation to $v_0 = a = 0$, which must be positive. Simply let $a = \varepsilon_3$. Then $v_0 = \varepsilon_3$ with $0 < \varepsilon_3 \ll \varepsilon_2$ yields $0 < v_0 \ll -v_1 \ll v_2 \ll -v_3$, provided that $0 < \varepsilon_3 \ll \varepsilon_2 \ll \varepsilon_1$.

As a numerical example, let $c = d = 1/2$, and choose the exact perturbations as $\varepsilon_1 = \frac{1}{10}$,

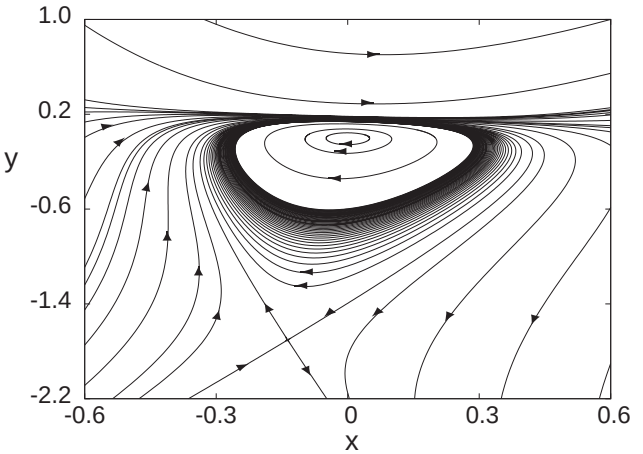

Fig. 1. The phase portrait of system (17) having three small limit cycles around the origin, for $a = 0.00000002$, $b = 0.0002$, $c = 0.5$, $d = 0.5$, $e = 7.6$.

$\varepsilon_2 = \frac{1}{5000}$, $\varepsilon_3 = \frac{1}{50000000}$. Then, executing the Maple program in [Yu, 1998] (with $a = 0$) yields the first equation of the normal form (14) up to term r^7 as

$$\begin{aligned}\dot{r} &= r(v_0 + v_1 r^2 + v_2 r^4 + v_3 r^6)\\ &= r\left(\frac{1}{50000000} - \frac{3}{80000}r^2 + \frac{56673782999}{4800000000000}r^4\right.\\ &\quad \left. - \frac{109954124078235019935229 3}{13824000000000000000000000}r^6\right),\end{aligned}$$

from which solving $\dot{r} = 0$ we obtain three positive roots: $r_1 = 0.025829\cdots$, $r_2 = 0.059536\cdots$ and $r_3 = 0.103114\cdots$, which approximate the amplitudes of the three small limit cycles bifurcating from the origin, as shown in Fig. 1.

3. Dynamical Analysis of Systems (3)–(7)

In this section, we consider the five predator–prey models (3)–(7) with different functional responses $p(x)$ and show that they may exhibit bifurcation of limit cycles, depending on the feasible values of the system parameters. In order to simplify the analysis, we first use state scaling and time scaling to change these systems to dimensionless forms with fewer parameters. For example, for system (3), taking the state scaling: $x = KX$, $y = \frac{r}{m}Y$ and time scaling $\tau = rt$, we obtain the following simple dimensionless system,

$$\text{System A}_\text{i}: \begin{cases}\dot{X} = X(1 - X - Y),\\ \dot{Y} = Y(CX - D),\end{cases} \tag{18}$$

where dot is still used for the differentiation $\frac{d}{d\tau}$ for simplicity, and the two new parameters are: $C = \frac{mK}{r}c$ and $D = \frac{1}{r}d$. Hence, the parameter numbers are reduced from five to two, greatly simplifying the analysis and computation. Note that the same time scaling, $\tau = rt$, and the same definition of the new parameter, $D = \frac{1}{r}d$, are applied to all the five systems (3)–(7).

In the following, without presenting details, we list the dimensionless equations corresponding to the other four systems, with the scaling given and new parameters defined.

$$\text{System A}_\text{ii}: \begin{cases}\dot{X} = X\left(1 - X - \dfrac{Y}{A + X}\right),\\ \dot{Y} = Y\left(\dfrac{CX}{A + X} - D\right),\end{cases} \tag{19}$$

where the scaling and new parameters are given by $x = KX$, $y = \frac{rK}{m}Y$, $A = \frac{1}{K}a$, $C = \frac{m}{r}c$.

$$\text{System A}_\text{iii}: \begin{cases}\dot{X} = X\left(1 - X - \dfrac{XY}{AX^2 + BX + 1}\right),\\ \dot{Y} = Y\left(\dfrac{CX^2}{AX^2 + BX + 1} - D\right),\end{cases} \tag{20}$$

where $x = KX$, $y = \frac{r}{mK}Y$, $A = K^2 a$, $B = Kb$, $C = \frac{mK^2}{r}c$.

$$\text{System B}_\text{i}: \begin{cases}\dot{X} = X(1 - M - X),\\ \dot{Y} = X - DY,\end{cases} \tag{21}$$

where $x = KX$, $y = \frac{mcK}{r}Y$, $M = \frac{1}{r}m$.

$$\text{System B}_\text{ii}: \begin{cases}\dot{X} = X\left(1 - X - \dfrac{MY}{X + Y}\right),\\ \dot{Y} = Y\left(\dfrac{CX}{X + Y} - D\right),\end{cases} \tag{22}$$

where $x = KX$, $y = \frac{K}{a}Y$, $M = \frac{1}{ar}m$, $C = \frac{m}{r}c$.

Note that all the normalized parameters are positive, except for B which may take zero and negative values, provided $B > -2\sqrt{A}$. In the following, we first consider the well-posedness of the solutions of the five predator–prey systems, and have the following result.

Theorem 1. *The solutions of the five predator–prey systems (18)–(22) [or the original systems (3)–(7)] are positive provided the initial conditions are positive. Moreover, the solutions are bounded.*

Proof. We choose system A_{iii} given by (20) as an example to show the positivity of the solutions, and other systems can follow the same approach. Using the method of constant variations, we can write the general solution of system A_{iii} with the initial value $X(0), Y(0)$ in the form of

$$X(\tau) = X(0)\exp\left\{\int_0^\tau \left[1 - X(s) - \frac{X(s)Y(s)}{AX^2(s) + BX(s) + 1}\right] ds\right\},$$

$$Y(\tau) = Y(0)\exp\left\{\int_0^\tau \left[\frac{CX^2(s)}{AX^2(s) + BX(s) + 1} - D\right] ds\right\},$$

which clearly shows that $X(\tau) > 0$, $Y(\tau) > 0$ for any $\tau > 0$ if $X(0) > 0$ and $Y(0) > 0$.

To show the boundedness of solutions of these systems, we define a triangular trapping region in the first quadrant of the X–Y plane, bounded by the X-axis, the Y-axis, and the line L, described by

$$\mathrm{L}: \quad 0 = F = \begin{cases} X + \dfrac{1}{C}Y - 1 - \dfrac{1}{4D}, & \text{for Systems } A_i,\ A_{ii},\ A_{iii}; \\ X + MY - 1 - \dfrac{1}{4D}, & \text{for System } B_i; \\ X + \dfrac{M}{C}Y - 1 - \dfrac{1}{4D}, & \text{for System } B_{ii}. \end{cases} \tag{23}$$

It is obvious that both the X-axis and Y-axis are invariant lines. So what we need to prove is just $\frac{dF}{d\tau} < 0$ on the right side of the line L (including the line). For example, for systems A_i, A_{ii} and A_{iii}, we obtain

$$\frac{dF}{d\tau} = \dot{X} + \frac{1}{C}\dot{Y} = X(1 - X) - \frac{D}{C}Y$$

$$= -\left(X - \frac{1}{2}\right)^2 - \frac{D}{C}\left(Y - \frac{C}{4D}\right) < 0,$$

for either $X > 1$ or $Y > \frac{C}{4D}$, implying that the trajectories move towards this region when crossing the line L, and thus the defined triangular region indeed attracts all the solutions of the system. ■

In the following subsections, we use the dimensionless equations (18)–(22) to study the dynamics of the five systems, and pay particular attention on the bifurcation of limit cycles due to Hopf and generalized Hopf bifurcations.

3.1. *Systems* A_i, B_i: *No limit cycles*

In this subsection, we consider the systems A_i and B_i, and show that they cannot exhibit bifurcation of limit cycles. It should be noted that if the logistic term $X(1 - X)$ in the systems (or $rx(1 - \frac{x}{K})$ in the original systems) is reduced to the linear term X (or rx), it is easy to show that these two systems become integrable (with an integrating factor $\frac{1}{XY}$, or $\frac{1}{xy}$ for the original systems). In other words, under this condition, these two systems will have first integrals, implying that all solutions of the systems are periodic but not isolated. Hence, there do not exist limit cycles.

3.1.1. *System* A_i

First, consider system A_i given by (18). The equilibrium solutions of this system can be easily found by setting $\dot{X} = \dot{Y} = 0$ as

$$\mathrm{E}_0: \quad (X_0, Y_0) = (0, 0);$$

$$\mathrm{E}_1: \quad (X_1, Y_1) = (1, 0);$$

$$\mathrm{E}_2: (X_2, Y_2) = \left(\frac{D}{C}, 1 - \frac{D}{C}\right), \quad (C > D).$$

We have the following theorem.

Theorem 2. *For system* A_i, *the equilibrium* E_0 *is a saddle*; *the equilibrium* E_1 *is globally asymptotically stable for* $C \le D$, *and usable for* $C > D$ *for which the equilibrium* E_2 *exists and is globally asymptotically stable. There is no bifurcation of limit cycles, nor is B–T bifurcation possible.*

Proof. It is easy to see that the condition $C > D$ on the equilibrium E_2 is to guarantee the positive values of Y. Otherwise, Y is extinct, resulting in $X = 0$ or $X = 1$. To find the stability of the equilibrium solutions, evaluating the Jacobian of the system at the three equilibria yield

$$J_0 = \begin{bmatrix} 1 & 0 \\ 0 & -D \end{bmatrix}, \quad J_1 = \begin{bmatrix} -1 & -1 \\ 0 & C-D \end{bmatrix},$$

$$J_2 = \begin{bmatrix} -\dfrac{D}{C} & -\dfrac{D}{C} \\ C-D & 0 \end{bmatrix},$$

which clearly indicate that E_0 is a saddle; E_1 is a saddle when $C > D$, and a stable node when $C < D$; and E_2 is a stable node (or focus) when $C > D$. When $C = D$, E_1 and E_2 coincide and become a degenerate stable node (which needs a simple analysis on the center manifold). Therefore, there is no Hopf bifurcation which can occur from any of the three equilibrium solutions. It is also obvious that B–T bifurcation is not possible from any of the three equilibria since it needs a double zero eigenvalue at the critical point.

To rule out other possibility of limit cycle bifurcations, we prove that E_1 is globally asymptotically stable when $C \le D$, and E_2 exists and is globally asymptotically stable when $C > D$. For the equilibrium E_1, we construct the Lyapunov function,

$$V_1(X, Y) = X - 1 - \ln X + \frac{1}{C}Y.$$

Differentiating V_1 with respect to time along the solution trajectories of system (18) yields

$$\begin{aligned} \left.\frac{dV_1}{d\tau}\right|_{(18)} &= \left(1 - \frac{1}{X}\right)\dot{X} + \frac{1}{C}\dot{Y} \\ &= (X-1)(1-X-Y) + \frac{1}{C}Y(CX - D) \\ &= -(X-1)^2 - Y\left(\frac{D}{C} - 1\right) \\ &\le 0, \quad \text{for } C \le D. \end{aligned}$$

When $C < D$, $\frac{dV_1}{d\tau}|_{(18)} = 0$ if and only if $(X, Y) = (1, 0)$. When $C = D$, $\frac{dV_1}{d\tau}|_{(18)} = 0$ if and only if $X = 1$ for which the first equation of (18) implies $Y = 0$. Hence, by applying the LaSalle's invariant principle, we have shown that the equilibrium E_1 is attractive and so (due to its local stability for $C < D$) is globally asymptotically stable for $C \le D$.

To prove the global stability for E_2, we similarly construct a Lyapunov function,

$$\begin{aligned} V_2(X, Y) = X - X_2 - X_2 \ln\left(\frac{X}{X_2}\right) \\ + \frac{1}{C}\left[Y - Y_2 - Y_2 \ln\left(\frac{Y}{Y_2}\right)\right]. \end{aligned}$$

Then, we have

$$\begin{aligned} \left.\frac{dV_2}{d\tau}\right|_{(18)} &= \left(1 - \frac{X_2}{X}\right)\dot{X} + \frac{1}{C} + \frac{1}{C}\left(1 - \frac{Y_2}{Y}\right)\dot{Y} \\ &= (X - X_2)(1 - X - Y) \\ &\quad + \frac{1}{C}(Y - Y_2)(CX - D) \\ &= -\left(X - \frac{D}{C}\right)^2 \le 0, \end{aligned}$$

which indicates that $\frac{dV_2}{d\tau}|_{(18)} = 0$ if and only if $X = \frac{D}{C}$; otherwise $\frac{dV_2}{d\tau}|_{(18)} < 0$. When $X = \frac{D}{C}$, $\dot{Y} = 0$ and it follows from the first equation of (18) that $Y = 1 - \frac{D}{C}$. Thus, with the LaSalle's invariant principle, we have shown that the equilibrium E_2 is attractive, and so globally asymptotically stable for $C > D$. Therefore, no bifurcation of limit cycles is possible in system A_i. We may also use a Dulac function $g(X, Y) = \frac{1}{XY}$ to prove that for system A_i there do not exist limit cycles in the first quadrant of the X–Y plane. ■

3.1.2. *System* B_i

The analysis on the dimensionless system B_i [see Eq. (21)] is even simpler than that for system A_i since here the function $p(x)$ is linear. System (21) has two equilibrium solutions:

$$E_0: \ (X_0, Y_0) = (0, 0);$$

$$E_1: \ (X_1, Y_1) = \left(1 - M, \frac{1-M}{D}\right); \quad (0 < M < 1).$$

We have the following result for system B_i.

Theorem 3. *For system* B_i, *the equilibrium* E_0 *is a stable node when* $M > 1$, *and becomes a saddle when* $M < 1$ *for which the equilibrium* E_1 *exists and is a stable node. Moreover,* E_0 *is globally asymptotically stable when* $M \ge 1$ *and* E_1 *is globally asymptotically stable when* $M < 1$. *There is no bifurcation of limit cycles, nor is B–T bifurcation possible.*

Proof. A similar linear analysis based on the Jacobian of system (21) shows that E_0 is a stable node when $M > 1$, and a saddle when $M < 1$; while E_1 exists and is a stable node when $M < 1$. It is clear that B–T bifurcation is not possible from either E_0 or E_1. Moreover, one can apply the Lyapunov function, $V_0 = X + (M-1)Y$, to prove that the equilibrium E_0 is globally asymptotically stable when $M \geq 1$, since

$$\left.\frac{dV_0}{d\tau}\right|_{(21)} = \dot{X} + (M-1)\dot{Y}$$
$$= -X^2 - (M-1)DY \leq 0, \quad \text{for } M \geq 1.$$

It equals zero if and only if $(X, Y) = (0, 0)$ when $M > 1$. When $M = 1$, it equals zero for $X = 0$. Then, by the second equation of (21) we have $Y \to 0$ as $t \to +\infty$. This, with the LaSalle's invariant principle, shows that E_0 is attractive and so globally asymptotically stable for $M \geq 1$.

Having known that E_1 exists and is locally asymptotically stable when $M < 1$, we now prove that E_1 is globally asymptotically stable when $M < 1$. To achieve this, consider the Lyapunov function,

$$V_1 = X - X_1 - X_1 \ln\left(\frac{X}{X_1}\right) + \frac{1}{2}D(Y - Y_1)^2$$

for E_1, and differentiating it with respect to time and using (21) yields

$$\left.\frac{dV_1}{d\tau}\right|_{(21)} = \left(1 - \frac{X_1}{X}\right)\dot{X} + D(Y - Y_1)\dot{Y}$$
$$= (X - X_1)(1 - M - X) + D(Y - Y_1)(X - DY)$$
$$= -\left[(X - X_1) - \frac{D}{2}(Y - Y_1)\right]^2 - \frac{3}{4}D^2(Y - Y_1)^2$$
$$\leq 0.$$

It is easy to see that $\frac{dV_1}{d\tau}|_{(21)} = 0$ if and only if $(X, Y) = (X_1, Y_1)$. This shows that E_1 is attractive, and so it is globally asymptotically stable for $M < 1$. ■

3.2. *Systems* A_{ii}, B_{ii}: *One limit cycle*

In this subsection, we turn to systems A_{ii} and B_{ii}, which are described by the dimensionless equations (19) and (22), respectively. We shall show that with the restriction on the parameter values, each of the two systems can have only one limit cycle bifurcating from a Hopf critical point.

3.2.1. *System* A_{ii}

First, consider system A_{ii}. Equation (19) has three equilibrium solutions, given by

$$E_0: \ (X_0, Y_0) = (0, 0);$$
$$E_1: \ (X_1, Y_1) = (1, 0);$$
$$E_2: \ (X_2, Y_2) = \left(\frac{AD}{C - D}, \frac{AC[C - (A+1)D]}{(C-D)^2}\right), \quad (C > (A+1)D).$$

For this system, we have the following result.

Theorem 4. *For system* A_{ii}, *the equilibrium* E_0 *is a saddle, while* E_1 *is globally asymptotically stable when* $C \leq (A+1)D$ *in which case* E_2 *does not exist.* E_1 *becomes unstable when* $C > (A+1)D$ *for which* E_2 *exists. Hopf bifurcation can occur from* E_2 *at the critical point* $C_H = \frac{(A+1)D}{1-A}$ $(A < 1)$, *with the transversal condition* $T_{\text{trans}} = \frac{(1-A)^3}{4DA(1+A)} \neq 0$ *and is supercritical, leading to bifurcation of single stable limit cycle. B–T bifurcation is not possible.*

Proof. A simple linear analysis shows that E_0 is a saddle, while E_1 is a stable node when $C < (A+1)D$ in which case E_2 does not exist. When $C > (A+1)D$, E_1 becomes unstable and E_2 emerges to exist. Hence, there is no Hopf bifurcation which can occur from E_1, and in fact, it can be shown that E_1 is globally asymptotically stable for $C \leq (A+1)D$. To achieve this, consider the Lyapunov function,

$$V_1 = X - 1 - \ln X + \frac{1}{AD}Y,$$

from which we obtain

$$\left.\frac{dV_1}{d\tau}\right|_{(19)} = \left(1 - \frac{1}{X}\right)\dot{X} + \frac{1}{AD}\dot{Y}$$
$$= -(X-1)^2 - [(A+1)D - C]\frac{XY}{AD(A+X)}$$
$$\leq 0, \quad \text{for } C \leq (A+1)D$$

and $\frac{dV_1}{d\tau}|_{(19)} = 0$ if and only if $(X, Y) = (1, 0)$ for $C < (A+1)D$. When $C = (A+1)D$, $\frac{dV_1}{d\tau}|_{(19)} = 0$ if and only if $X = 1$ for which the first equation of (19) yields $Y \to 0$ as $t \to +\infty$. Thus, with the

LaSalle's invariant principle, we have shown that E_1 is attractive, and so globally asymptotically stable.

Now, we investigate the possibility of Hopf bifurcation from the equilibrium E_2. Under the condition $C > (A+1)D$, the equilibrium E_2 exists. Evaluating the Jacobian of system (19) at E_2 yields the trace and determinant:

$$\mathrm{Tr}(J_2) = \frac{D}{C(C-D)}[(1-A)C - (A+1)D],$$

$$\det(J_2) = \frac{D}{C}[(C-(A+1)D] > 0 \quad (\text{due to } C > (A+1)D).$$

Thus, the equilibrium E_2 is stable for $A \geq 1$ or for $A < 1$ when $C < \frac{(A+1)D}{1-A}$; unstable for $A < 1$ when $C > \frac{(A+1)D}{1-A}$. At the critical point, $C_H = \frac{(A+1)D}{1-A}$, $(A < 1)$, Hopf bifurcation occurs from E_2. Note that B–T bifurcation cannot happen since $\det(J_2) > 0$ when E_2 exists. Moreover, $T_{\text{trans}} = \frac{1}{2}\frac{d\,\mathrm{Tr}(J_2)}{dC}\big|_{C=C_H} = \frac{(1-A)^3}{4DA(1+A)} \neq 0$.

In the following, we want to find how many limit cycles can exist near the equilibrium E_2 due to the Hopf bifurcation. In general, we have three free parameters, A, C and D, and might get maximal three small-amplitude limit cycles if no restriction is posed on the parameters. We need to find the focus values v_k's from the normal form computation [see (14)]. To simplify the computation, we first introduce an additional time scaling $\tau = (A+X)\tau_1$ into (19) and then a linear transformation $X = x_1$, $Y = -\frac{2\omega_c}{1-A}x_2$, where $\omega_c = \frac{A+1}{2}\sqrt{AD}$, into the resulting equation to obtain the following system:

$$\begin{aligned}\dot{x}_1 &= \omega_c x_2 - \frac{1-A}{2}x_1^2 + \frac{2\omega_c}{1-A}x_1x_2 - x_1^3 \\ &\equiv f(x_1, x_2),\end{aligned}$$

$$\begin{aligned}\dot{x}_2 &= -\omega_c x_1 + \frac{2}{1-A}x_1x_2 \\ &\equiv g(x_1, x_2),\end{aligned}$$

in which the linear part is in Jordan canonical form. Finally, we use the formula of computing the first focus value at the critical point, $(x_1, x_2) = (0,0)$ (e.g. see [Guckenheimer & Holmes, 1993]) to obtain

$$\begin{aligned}v_1 &= \frac{1}{16}\left[\frac{\partial^3 f}{\partial x_1^3} + \frac{\partial^3 f}{\partial x_1 x_2^2} + \frac{\partial^3 g}{\partial x_1^2 x_2} + \frac{\partial^3 g}{\partial x_2^3}\right] \\ &\quad - \frac{1}{16\omega_c}\left[\frac{\partial^2 f}{\partial x_1 x_2}\left(\frac{\partial^2 f}{\partial x_1^2} + \frac{\partial^2 f}{\partial x_2^2}\right)\right. \\ &\quad \left. - \frac{\partial^2 g}{\partial x_1 x_2}\left(\frac{\partial^2 g}{\partial x_1^2} + \frac{\partial^2 g}{\partial x_2^2}\right) - \frac{\partial^2 f}{\partial x_1^2}\frac{\partial^2 g}{\partial x_1^2} + \frac{\partial^2 f}{\partial x_2^2}\frac{\partial^2 g}{\partial x_2^2}\right] \\ &= \frac{1}{16}\frac{\partial f^3}{\partial x_1^3} - \frac{1}{16\omega_c}\frac{\partial f^2}{\partial x_1 x_2}\frac{\partial f^2}{\partial x_1^2} \\ &= \frac{-6}{16} - \frac{1}{16\omega_c}\left[\frac{2\omega_c}{1-A} \times \left(-\frac{2(1-A)}{2}\right)\right] \\ &= -\frac{1}{4}.\end{aligned}$$

(Executing the Maple program in [Yu, 1998] on the above system yields the same result.) A constant v_1, irrelative to system parameters, clearly indicates that system A_{ii} can have only one small-amplitude limit cycle bifurcating from the equilibrium E_2 due to Hopf bifurcation. Moreover, the negative sign of v_1 indicates that the Hopf bifurcation is supercritical and so the bifurcating limit cycle is stable. ■

3.2.2. *System* B_{ii}

Unlike system A_{ii}, system B_{ii} which is given in (22) has only two equilibrium solutions:

$$E_1: \ (X_1, Y_1) = (1, 0);$$

$$E_2: \ (X_2, Y_2) = \left(1 - \frac{M}{C}(C-D), \frac{1}{D}(C-D)\left[1 - \frac{M}{C}(C-D)\right]\right), \quad \left(0 < M < \frac{C}{C-D}\right).$$

It should be noted that the point $(X, Y) = (0,0)$ [or $(x, y) = (0,0)$ for the original system (7)] cannot be an equilibrium solution of the system, nor can be chosen as an initial point, since $\lim_{X\to 0, Y\to 0}\frac{XY}{X+Y}$ does not exist along the line $X + Y = 0$.

For this system, we have the following result.

Theorem 5. *For system* B_{ii}, *the equilibrium* E_1 *is globally asymptotically stable for* $C < D$, *and unstable for* $C > D$ *for which* E_2 *exists.* E_2 *is asymptotically stable when* $M \in (0, \frac{C(C+CD-D^2)}{C^2-D^2})$ *if* $C \in (D, D+1)$, *or when* $M \in (0, \frac{C}{C-D})$ *if* $C \geq D+1$; *and unstable when* $M \in (\frac{C(C+CD-D^2)}{C^2-D^2}, \frac{C}{C-D})$ *if* $C \in (D, D+1)$, *with the transversal condition* $T_{\text{trans}} = \frac{C^2-D^2}{2C^2} \neq 0$. *Hopf bifurcation occurs from*

E_2 *at* $M_H = \frac{C(C+CD-D^2)}{C^2-D^2}$ *for* $C \in (D, D+1)$, *and the Hopf bifurcation is supercritical, leading to stable limit cycles. B–T bifurcation is not possible.*

Proof. By a linear analysis, we can show that E_1 is a stable node when $C < D$ for which E_2 (physically) does not exist; and E_1 is unstable (a saddle) for $C > D$ in which case E_2 exists. Moreover, we can prove that E_1 is globally asymptotically stable for $C < D$. To achieve this, construct the Lyapunov function,

$$V_1 = \frac{1}{2}(X-1)^2 + \frac{M}{D-C}Y,$$

from which we obtain

$$\begin{aligned}\left.\frac{dV_1}{d\tau}\right|_{(22)} &= (X-1)\dot{X} + \frac{M}{D-C}\dot{Y} \\ &= (X-1)X\left(1 - X - \frac{MY}{X+Y}\right) \\ &\quad + \frac{M}{D-C}Y\left(\frac{CX}{X+Y} - D\right) \\ &= -X(X-1)^2 - \frac{MY}{X+Y}\left[X^2 + \frac{DY}{D-C}\right] \\ &\leq 0 \quad \text{for } C < D\end{aligned}$$

and $\frac{dV_1}{d\tau}|_{(22)} = 0$ if and only if $(X, Y) = (1, 0)$ (noticing that $(X, Y) = (0, 0)$ is not allowed for the solution of the system). This shows that E_1 is attractive and, together with its local asymptotic stability, we can conclude that E_1 is globally asymptotically stable for $C < D$.

Next, consider the stability of E_2. Evaluating the Jacobian of (22) at E_2 yields

$$\begin{aligned}\mathrm{Tr}(J_2) &= \frac{(C^2-D^2)M - C(C+DC-D^2)}{C^2}, \\ \det(J_2) &= \frac{D(C-D)[C-M(C-D)]}{C^2}.\end{aligned}$$

Hence, $\det(J_2) > 0$ for $M < \frac{C}{C-D}$, $(C > D)$, implying that B–T bifurcation cannot happen from the equilibrium E_2. Using $\mathrm{Tr}(J_2)$, we obtain the following stability conditions for E_2:

$$E_2 \text{ is stable if } \begin{cases} M < \dfrac{C(C+DC-D^2)}{C^2-D^2}, & \text{for } D < C < D+1, \\ M < \dfrac{C}{C-D} \Rightarrow M < \dfrac{C(C+DC-D^2)}{C^2-D^2}, & \text{for } C \geq D+1, \end{cases}$$

$$E_2 \text{ is unstable if } \frac{C(C+DC-D^2)}{C^2-D^2} < M < \frac{C}{C-D}, \quad \text{for } D < C < D+1.$$

Thus, when $D < C < D+1$, there exists a Hopf critical point at $M_H = \frac{C(C+DC-D^2)}{C^2-D^2}$. Moreover, the transversal condition is given by $T_{\text{trans}} = \frac{1}{2}\frac{d\,\mathrm{Tr}(J_2)}{dM}|_{M=M_H} = \frac{C^2-D^2}{2C^2} \neq 0$. To find the stability of the bifurcating limit cycle, applying an additional time scaling $\tau = (X+Y)\tau_1$ with a linear transformation and then executing the Maple program [Yu, 1998] we obtain the first-order focus value,

$$\begin{aligned}v_1 &= -\frac{(C-D)(D+1-C)}{8[C+D(C-D)]} \\ &< 0, \quad \text{for } D < C < D+1\end{aligned}$$

and thus system B_{ii} can have only one small-amplitude limit cycle bifurcating from E_2 due to Hopf bifurcation. The Hopf bifurcation is supercritical, yielding stable limit cycles. ■

3.3. *System* A_{iii}: *Two limit cycles*

Now we turn to system A_{iii} given by (20). Note that for this system the parameters A, C and D take positive values, while B may take positive, zero or negative values, provided $B > -2\sqrt{A}$. We will show that this system can have multiple Hopf bifurcation points to yield one limit cycle, and bifurcation of maximal two limit cycles for certain parameter values.

3.3.1. *Equilibrium solutions*

First, we consider equilibrium solutions of system A_{iii}. This system also has three equilibrium solutions, given by

$$E_0: \ (X_0, Y_0) = (0, 0);$$

$$\mathrm{E}_1: \quad (X_1, Y_1) = (1, 0);$$

$$\mathrm{E}_2: \quad (X_2, Y_2) = \left(X_2, \frac{C}{D} X_2(1 - X_2)\right); \quad (0 < X_2 < 1),$$

where X_2 is determined from the following quadratic polynomial equation:

$$F_1 = (C - AD)X_2^2 - BDX_2 - D = 0, \qquad (24)$$

which has the solutions,

$$X_2^{\pm} = \frac{1}{2(C - AD)}(BD \pm \sqrt{\Delta}), \quad \text{where}$$

$$\Delta = B^2D^2 + 4D(C - AD). \qquad (25)$$

We need to consider two cases: $B \geq 0$ and $-2\sqrt{A} < B < 0$.

When $B \geq 0$, it is easy to see from (24) that the necessary condition for $F_1 = 0$ to have positive solutions of X_2 is $C > AD$, which guarantees $\Delta > 0$. Thus, $X_2^+ > 0$ but $X_2^- < 0$. So, when $B \geq 0$, the only positive solution is X_2^+ under the condition $C > AD$. We may plot the solution X_2, determined by $F_1 = 0$, on the C–X_2 plane, as shown in Fig. 2(a). It is seen from this figure that the graph $F_1 = 0$ is monotonic, which is confirmed by

$$\frac{dC}{dX_2} = -\frac{\sqrt{\Delta}}{X_2^2} < 0 \quad \text{for } X_2 > 0.$$

When $-2\sqrt{A} < B < 0$, define

$$C^* = D\left(A - \frac{1}{4}B^2\right) > 0, \qquad (26)$$

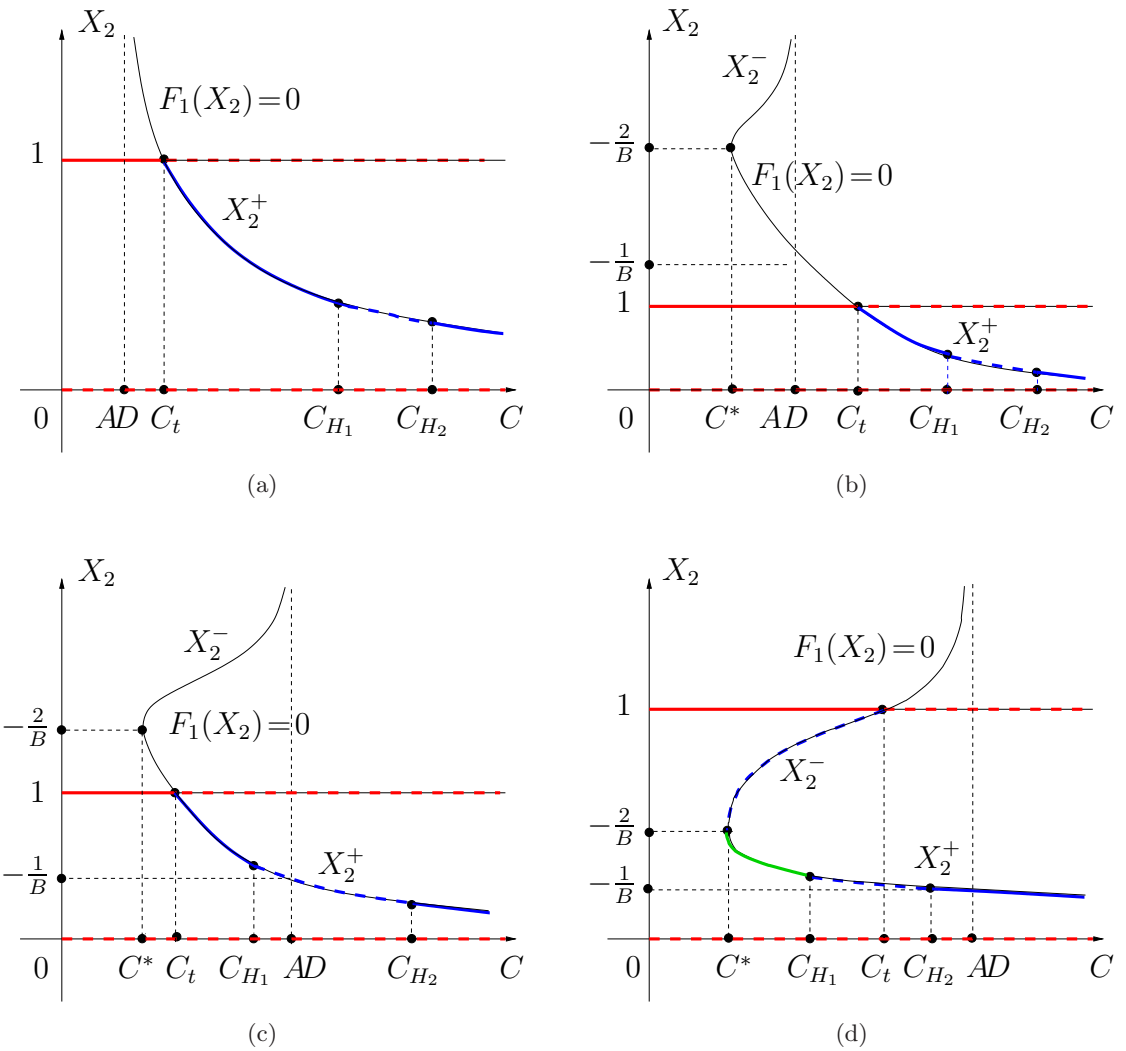

Fig. 2. Bifurcation diagrams for system $\mathrm{A_{iii}}$ when (a) $B \geq 0$, (b) $\max\{-2\sqrt{A}, -1\} < B < 0$, (c) $\max\{-2\sqrt{A}, -2\} < B < -1$, $A > \frac{1}{4}$ and (d) $-2\sqrt{A} < B < -2$, $A > 1$, with colored solid curves (lines) and dashed curves (lines) denoting stable and unstable equilibrium solutions, respectively. The negative part of X_2^- for $C > AD$ is not shown in the figures.

at which $X_2 = -\frac{2}{B}$. Then, $\Delta = 4D(C - C^*)$. In order to have real solutions for $X_2^{\pm}$, it requires that $\Delta \geq 0$, i.e. $C \geq C^*$, under which both solutions $X_2^{\pm}$ exist, and note that $X_2^+ < X_2^-$ for $C^* < C < AD$ but $X_2^+ > 0 > X_2^-$ for $C > AD$. Similarly, as shown in Figs. 2(b)–2(d), where X_2^- is not shown for $C > AD$, we can plot the solution X_2 for different values of $B \in (-2\sqrt{A}, 0)$. Further, if we consider C as a function of X_2, determined from $F_1 = 0$, it is easy to show that this function has a global minimum at the point $(C, X_2) = (C^*, -\frac{2}{B})$, and it is monotonically decreasing when $0 < X_2 < -\frac{2}{B}$, and monotonically increasing when $X_2 > -\frac{2}{B}$. This can be observed from Figs. 2(b)–2(d), where C^* is the minimum at the vertex of the graph of $F_1 = 0$. Moreover, it is easy to show that when $B < 0$, $X_2^- > 0$ for $C \in (C^*, AD)$, $X_2^- < 0$ for $C > AD$ and $\lim_{C-D\to 0^{\mp}} = \pm\infty$, as well as $X_2^+|_{C=AD} = -\frac{1}{B}$ and $\lim_{C\to+\infty} X_2^{\pm} = 0$.

Summarizing the above results gives the solutions for $X_2 > 0$:

$$X_2 = \begin{cases} X_2^+ = \dfrac{BD + \sqrt{\Delta}}{2(C - AD)}, & \text{for } B \geq 0,\ C > AD; \\ \qquad\qquad \text{or} \quad -2\sqrt{A} < B < 0,\ C \geq C^*; \\ X_2^- = \dfrac{BD - \sqrt{\Delta}}{2(C - AD)}, & \text{for } -2\sqrt{A} < B < 0, \\ \qquad\qquad C^* \leq C < AD. \end{cases} \tag{27}$$

It follows from (24) that on the C–X_2 plane, the curve $F_1 = 0$ intersects the line $X_2 = 1$ at the point $C = C_t$, where

$$C_t = (A + B + 1)D, \tag{28}$$

in which the subscript "t" denotes *transcritical bifurcation*. Thus, the part of the curve $F_1 = 0$ below the line $X_2 = 1$ corresponds to $X_2 < 1$. It is easy to see that when $B = -1$, $AD = C_t$, and when $-2 < B < 0$, $X_2^- > 1$. So $X_2^- < 1$ can exist only if $-2\sqrt{A} < B < -2$. $B = -2$ is a critical point at which $C^* = C_t$, and $X_2^- = 1$.

3.3.2. *Stability of the equilibria and Hopf bifurcations*

For convenience in studying the stability of the equilibria $\mathrm{E}_0, \mathrm{E}_1$ and E_2, and Hopf bifurcations arising from E_2, we define the equilibria $\mathrm{E}_2^{\pm} : (X_2^{\pm}, Y_2^{\pm})$, the Hopf critical points as C_H or C_{H_1}, C_{H_2}, and the following notations:

$$\begin{aligned} A_H &= B(B+1) + \frac{B+1}{B+3}, \\ B_H &= A - 3A^{2/3}, \\ B_H^k &= \min\{k, B_H\}, \quad k = 0, -2, -3, -4 \end{aligned} \tag{29}$$

and

$$\begin{aligned} \gamma_1 :&\ \{8 < A < A_H, -4 < B < B_H^{-3}\}, \\ \gamma_2 :&\ \{4 < A < A_H, -2\sqrt{A} < B < -4\} \\ &\cup \{8 < A < A_H, B = -4\} \\ &\cup \{A > A_H, -4 < B < B_H^{-3}\}, \\ \gamma_3 :&\ \{A > 9, B \leq -6\} \\ &\cup \left\{A < \frac{B^2}{B+6}, B > -6\right\}. \end{aligned} \tag{30}$$

Then, we have the following theorem.

Theorem 6. *For system* $\mathrm{A_{iii}}$, *the equilibrium* E_0 *is a saddle, and* E_2^- *is also a saddle when it exists for* $B \in (-2\sqrt{A}, -2]$ *and* $C \in (C^*, C_t)$. *The conditions for the stability of* E_1 *and* E_2^+, *Hopf bifurcation with nonzero transversality and bistable property are listed in Table 1, where the GAS, LAS, Stab LC,* BIS^1 *and* BIS^2 *respectively represent Globally Asymptotically Stable, Locally Asymptotically Stable, Stable Limit Cycle, Bistable with two equilibria, and Bistable with one equilibrium and one limit cycle.*

Remark 3.1. Figure 3 shows the partition of the parameters in the (A, B) plane, corresponding to Theorem 6, in which the regions where two Hopf bifurcations may occur are shaded by vertical lines, and one Hopf bifurcation shaded by horizontal lines. The numbers of bifurcating limit cycles are marked by ②, ① and ⓪. The region γ_1 is the dark shaded area, and the region γ_2 is the shaded area (including both vertical and horizontal lines) outside γ_1. The region γ_3 is below the curve $A = \frac{B^2}{B+6}$. It is easy to see that $\mathrm{BIS}^1 \in \{-2\sqrt{A} < B \leq -2\}$ and $\mathrm{BIS}^2 \in \gamma_1 \oplus \gamma_2 \backslash \gamma_3$. It should be noted that the conditions given in Fig. 3 must be combined with the condition on C given in the table to get the complete conditions for the stability of limit cycles and bistability. For example, for BIS^2 in the case of two limit cycles when $-2\sqrt{A} < B \leq -2$, the condition $(A, B) \in \gamma_1$ is not enough, and the other condition $C \in (C_{H_1}, C_{H_2})$ must be combined. Note that B–T

Table 1. Stability of E_1 and E_2^+, Hopf bifurcation and bistability of system A_{iii}.

Case	$B > \max\{-2\sqrt{A}, -2\}$		$-2\sqrt{A} < B \le -2$		
E_1	GAS for $C \in (0, C_t]$		GAS for $C \in (0, C^*]$ LAS for $C \in (C^*, C_t)$		
Hopf Cond	$A > 27$, $0 < B < B_H$ or $A > 10 + 6\sqrt{3}$, $-2 < B < B_H^0$	Otherwise	$A > 8$, $-4 < B < B_H^{-2}$	$A > 4$, $-2\sqrt{A} < B < -4$ or $A > 8$, $B = -4$	Otherwise
Hopf No	2	0	2	1	0
Stab LC	$C \in (C_{H_1}, C_{H_2})$		$C \in (C_{H_1}, C_{H_2})$	$(A, B) \notin \gamma_3$ $C \in (C^*, C_H)$	
E_2^+ (LAS)	$C \in (C_t, C_{H_1}) \cup (C_{H_2}, \infty)$	$C > C_t$	$C \in (C^*, C_{H_1}) \cup (C_{H_2}, \infty)$	$C > C_H$	$C > C^*$
BIS[1]	None		$(A, B) \in \gamma_1$, $C \in (C^*, C_{H_1}) \cup (C_{H_2}, C_t)$	$(A, B) \in \gamma_2$, $C \in (C_H, C_t)$	$C \in (C^*, C_t)$
BIS[2]	None		$(A, B) \in \gamma_1$, $C \in (C_{H_1}, C_{H_2})$	$(A, B) \in \gamma_2 \backslash \gamma_3$, $C \in (C^*, C_H)$	None

bifurcation can occur from the equilibrium E_2^+ when the saddle-node bifurcation and the Hopf bifurcation coincide when $B = -4$ and $C = D(A-4)$ $(A > 4)$. It can be shown that the B–T bifurcation can be codimension two or three. The detailed analysis on the B–T bifurcation is out of scope of this paper and we leave it as future work.

Proof. First, it is straightforward to apply a linear analysis to prove that E_0 is a saddle. To analyze the stability of E_1 and E_2, we need to consider two cases.

Case (i). $B \ge 0$. For this case, E_1 is a stable node when $C < C_t$ and it loses its stability at the critical point $C = C_t$, and then becomes a saddle for $C > C_t$. More precisely, we can show that E_1 is globally asymptotically stable for $C < C_t$ $(B \ge 0)$. In fact, in this case, $X_2^- < 0$, and the positive E_2^+ requires $X_2 < 1$ (due to $Y_2 > 0$) which in turn yields the condition $C > C_t$, and thus in this case, the system has a unique stable equilibrium E_1 when $C < C_t$.

Then, note that for $C < C_t$, both the X-axis and the Y-axis are solution trajectories with the boundary equilibrium $E_0 : (0,0)$ being a saddle, and another boundary equilibrium $E_1 : (1,0)$ being a stable node. It has been shown in Theorem 1 that a trapping region exists, attracting all trajectories of the system. Since there is only one stable equilibrium E_1 on the boundary of the trapping region, all trajectories will converge to E_1, showing that E_1 is globally asymptotically stable for $C < C_t = (A + B + 1)D$ when $B \ge 0$.

To study the stability of E_2, we solve the equation $F_1 = 0$ for C to obtain

$$C = \frac{D}{X_2^2}(AX_2^2 + BX_2 + 1) > 0, \tag{31}$$

because for $X_2 > 0$, we have

$$\frac{D}{X_2^2}(AX_2^2 + BX_2 + 1)$$

$$\begin{cases} > 0, \quad \text{if } B \ge 0, \\ = D\left(\dfrac{1}{X_2} + \dfrac{B}{2}\right)^2 + D\left(A - \dfrac{B^2}{4}\right) > 0, \\ \qquad\qquad \text{if } -2\sqrt{A} < B < 0, \end{cases}$$

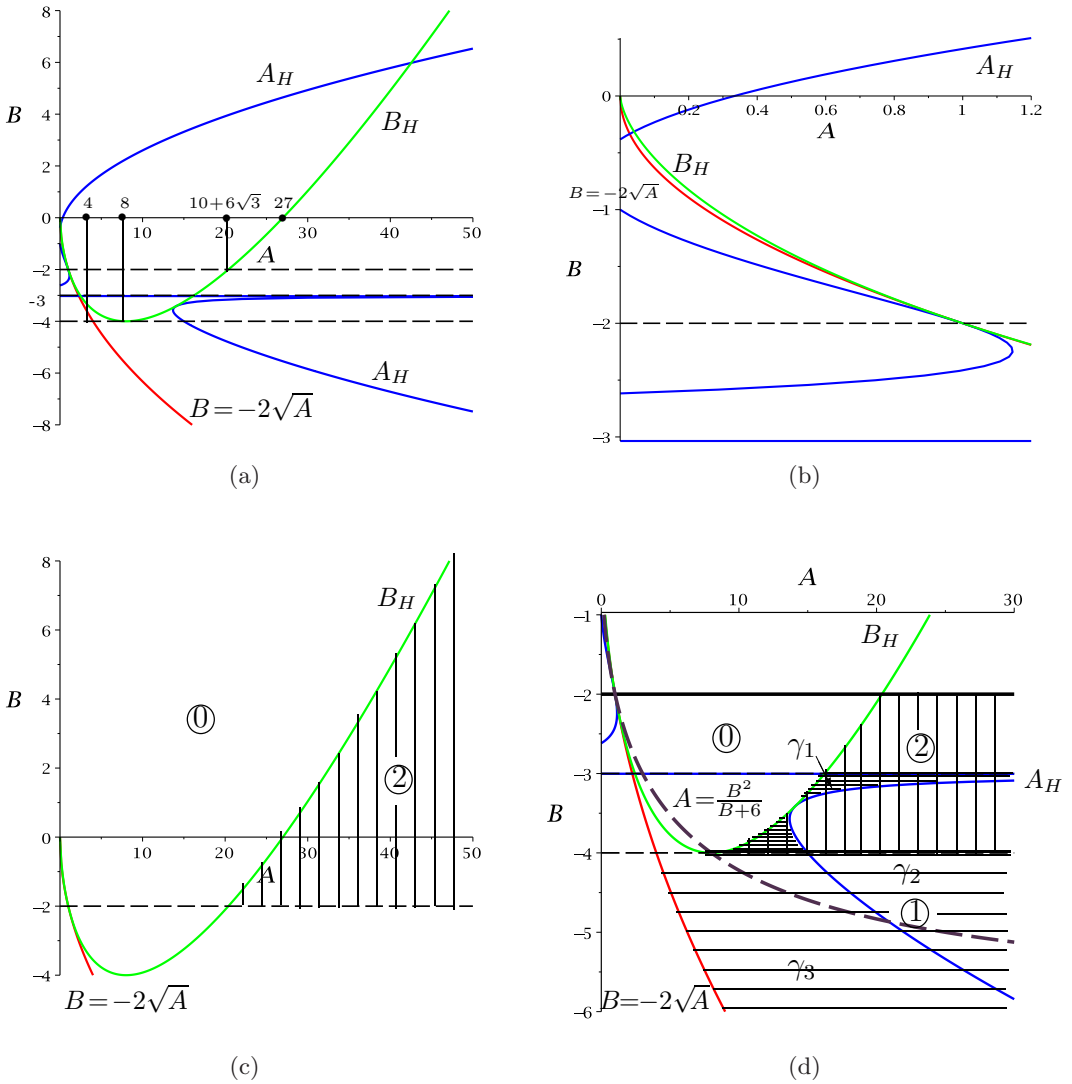

Fig. 3. Parameter partitions in (A, B) parameter plane: (a) the whole feasible parameter region above the half parabola (the red curve), (b) the zoomed area near the origin, (c) the region for $B > \max\{-2\sqrt{A}, -2\}$ and (d) the region for $-2\sqrt{A} < B \leq -2$.

which defines the minimum value of $C = C^*$ obtained at $X_2 = -\frac{2}{B}$ when $B \in (-2\sqrt{A}, 0)$. Then, evaluating the Jacobian of (20) at E_2 yields the trace and determinant, given by

$$\begin{aligned}\mathrm{Tr}(J_2) &= \frac{1}{AX_2^2 + BX_2 + 1} \\ &\quad \times [-2AX_2^3 + (A - B)X_2^2 - 1], \\ \det(J_2) &= \frac{D}{AX_2^2 + BX_2 + 1}(1 - X_2)(BX_2 + 2).\end{aligned} \tag{32}$$

Thus, when $B \geq 0$, it is easy to see that $\det(J_2) > 0$ for $0 < X_2 < 1$, and so the stability of E_2^+ is determined by the trace of J_2, namely, E_2^+ is asymptotically stable (unstable) if $\mathrm{Tr}(J_2) < 0$ ($\mathrm{Tr}(J_2) > 0$). This implies that B–T bifurcation cannot occur from the equilibrium E_2^+ for $B \geq 0$. Moreover, consider A as the bifurcation parameter such that $\mathrm{Tr}(J_2)|_{A=A_H} = 0$, where $A_H = \frac{1+BX_2^2}{X_2^2(1-2X_2)} > 0$. Then,

$$\begin{aligned}T_{\mathrm{trans}} &= \frac{1}{2}\frac{d\,\mathrm{Tr}(J_2)}{dA}\Big|_{A=A_H} \\ &= \frac{X_2^2(1 - X_2)(BX_2 + 2)}{2(A_H X_2^2 + BX_2 + 1)^2} \neq 0,\end{aligned}$$

showing that the transversality condition holds. This condition is also true for Case (ii) to be considered next.

Note that the factor of $\mathrm{Tr}(J_2)$ in the square bracket is a cubic polynomial in X_2. Thus, using the discriminator of the cubic polynomial factor of

$\mathrm{Tr}(J_2)$, given by

$$\mathrm{Disc} = \frac{1}{432A^4}[27A^2 + (B-A)^3], \tag{33}$$

we can determine the number of real solutions of $\mathrm{Tr}(J_2) = 0$ as follows:

$$\mathrm{Tr}(J_2) \text{ has } \begin{cases} 3 \text{ distinct real roots}, & \text{if Disc} < 0, \\ 1 \text{ real root}, & \text{if Disc} > 0, \\ 3 \text{ real roots with two being identical}, & \\ & \text{if Disc} = 0. \end{cases} \tag{34}$$

However, note that one of the real solutions of the equation $\mathrm{Tr}(J_2) = 0$ must be negative because $\mathrm{Tr}(J_2)|_{X_2=0} = -1$ and $\mathrm{Tr}(J_2)|_{X_2\to-\infty} = +\infty$. Moreover, noticing that

$$\lim_{X_2\to 1} \mathrm{Tr}(J_2) = \lim_{X_2\to 0^+} \mathrm{Tr}(J_2) = -1, \tag{35}$$

we know that for Disc < 0 there may exist none or two positive Hopf critical points on E_2^+; and so E_2^+ is stable either for $C \in [C_t, +\infty)$ or for $C \in [C_t, C_{H_1}) \cup (C_{H_2}, +\infty)$, where C_{H_1} and C_{H_2} denote two Hopf critical points. The case Disc > 0 generates a negative solution, implying that no Hopf bifurcation occurs and so E_2^+ is stable for the whole interval $C \in [C_t, +\infty)$ if Disc > 0. Further, note that the case Disc $= 0$ is actually a special case, which characterizes the coincidence of two Hopf critical points $C_{H_1} = C_{H_2} = C_H$, and thus can be considered the same as the case Disc > 0, since E_2^+ is stable for the whole interval $C \in (C_t, \infty)$ except for one isolated point $C = C_H$. Summarizing the above discussions we have that

No Hopf critical points exist on E_2^+ if Disc ≥ 0,

Two Hopf critical points exist on E_2^+ if Disc < 0.

Therefore, in order to have Hopf bifurcations from E_2^+, the equation $\mathrm{Tr}(J_2) = 0$ must have positive solutions for $X_2 \in (0,1)$. In other words, the positive Hopf critical points should satisfy $X_2 \in (0,1)$. To investigate whether $\mathrm{Tr}(J_2) = 0$ has such solutions, we rewrite $\mathrm{Tr}(J_2)$ given in (32) as

$$\mathrm{Tr}(J_2) = 1 - 2X_2 - \frac{(1-X_2)(BX_2+2)}{AX_2^2 + BX_2 + 1}. \tag{36}$$

It is easy to see that Eq. (36) may have positive solutions for $X_2 \in (0,1)$ only if $0 < X_2 < \frac{1}{2}$. In the following, we will show that for $B \geq 0$ together with the condition Disc < 0, namely $B < B_H$, the equation $\mathrm{Tr}(J_2) = 0$ always has two positive real solutions, say, $X_{2a}, X_{2b} \in (0, \frac{1}{2})$. Suppose there exist such two values X_{2a} and X_{2b}, corresponding to the two Hopf critical points, we may find possible values of A and B satisfying the equation $\mathrm{Tr}(J_2) = 0$. In fact, for these two values X_{2a} and X_{2b}, we obtain two equations from (36) and then solving the two equations for A and B yields

$$A = \frac{X_{2a} + X_{2b}}{2X_{2a}^2 X_{2b}^2},$$

$$B = \frac{X_{2a} + X_{2b} - 2X_{2a}^2 - 2X_{2b}^2 - 2X_{2a}X_{2b}}{2X_{2a}^2 X_{2b}^2}.$$

When $B \geq 0$, Disc < 0 implies $A > 27$. We use the above two equations to obtain

$$\frac{B}{A} = 1 - 2(X_{2a} + X_{2b}) + \frac{2X_{2a}X_{2b}}{X_{2a} + X_{2b}} \equiv \mathrm{Eq}(X_{2a}, X_{2b}). \tag{37}$$

Thus, for $0 < B < B_H$, we have $0 \leq \frac{B}{A} < \frac{B_H}{A} \in (0,1)$ for $A > 27$. On the other hand, $\mathrm{Eq}(X_{2a}, X_{2b})$ can equal any values in $(0,1)$ for suitable values of $X_{2a}, X_{2b} \in (0, \frac{1}{2})$ since

$$\mathrm{Eq}(0,0) = 1, \quad \mathrm{Eq}\left(\frac{1}{3}, \frac{1}{3}\right) = 0,$$

$$\frac{\partial \mathrm{Eq}}{\partial X_{2a}} = -2\left[1 - \left(\frac{X_{2b}}{X_{2a} + X_{2b}}\right)^2\right] < 0, \quad \text{for } X_{2a}, X_{2b} \in \left(0, \frac{1}{2}\right),$$

$$\frac{\partial \mathrm{Eq}}{\partial X_{2b}} = -2\left[1 - \left(\frac{X_{2a}}{X_{2a} + X_{2b}}\right)^2\right] < 0, \quad \text{for } X_{2a}, X_{2b} \in \left(0, \frac{1}{2}\right).$$

Note that the graph $F_1 = 0$ is continuous for $X_2 \in (0,1)$ [see Fig. 2(a)], and the equation $\mathrm{Tr}(J_2) = 0$ can have positive solutions only for $X_2 \in (0, \frac{1}{2})$. Therefore, when Disc < 0, the solutions X_{2a} and X_{2b} for the two Hopf critical points must be obtained in the interval $X_2 \in (0, \frac{1}{2})$. Summarizing the above discussions we conclude that there exist two Hopf bifurcations from E_2^+ when $A > 27$ and $0 \leq B < B_H$.

The bifurcation diagram for this case $B \geq 0$ is depicted in Fig. 2(a), which shows two Hopf critical points (a numerical example will be given in Sec. 4), with C_t denoting the transcritical bifurcation point,

and C_{H_1} and C_{H_2} representing two Hopf critical points.

Case (ii). $-2\sqrt{A} < B < 0$. First, consider E_1. Evaluating the Jacobian at E_1 yields the eigenvalues -1 and $\frac{C}{A+B+1} - D$, where $A+B+1 > A-2\sqrt{A}+1 = (\sqrt{A}-1)^2 \geq 0$. Thus, like Case (i), we can still conclude that E_1 is asymptotically stable (unstable) when $C < C_t$ ($C > C_t$).

The analysis on stability of E_2 is more complicated for this case since now we have two possible equilibria: E_2^+ and E_2^-. The solution branch X_2^+ is below the solution branch X_2^-, as shown in Figs. 2(b)–2(d). However, we can still use (32) to determine the stability of E_2, but need to distinguish E_2^- from E_2^+ by using $X_2 = -\frac{2}{B}$ at the vertex as a turning point.

First note that when $0 < X_2 < 1$ and $-2 \leq B < 0$, we have $BX_2 + 2 \geq 0$. Hence, for $\max\{-2\sqrt{A}, -2\} < B < 0$, it follows that $X_2^- > -\frac{2}{B} > 1$ [see Figs. 2(b) and 2(c)] which has no biological meaning, and from (32) that $\det(J_2) > 0$ on E_2^+. Thus, similar to the case $B \geq 0$, the stability of E_2^+ is determined by the sign of $\mathrm{Tr}(J_2)$. We can also use (33) and (34) to determine the number of Hopf critical points. No Hopf bifurcation can occur if Disc ≥ 0; while when Disc < 0, it is slightly different from the case $B \geq 0$. For $\max\{-2\sqrt{A}, -2\} < B < 0$ together with Disc < 0, we have $\max\{-2\sqrt{A}, -2\} < B < B_H^0$, which requires $A > 10 + 6\sqrt{3}$, since

$$\begin{aligned} B_H + 2\sqrt{A} &= A - 3A^{2/3} + 2\sqrt{A} \\ &= \sqrt{A}(A^{1/6} - 1)^2(A^{1/6} + 2) > 0 \end{aligned}$$

for $A > 0$, $(A \neq 1)$; and

$$\begin{aligned} B_H + 2 &= A - 3A^{2/3} + 2 \\ &= (A^{1/3} + \sqrt{3} - 1)(A^{1/3} - 1) \\ &\quad \times (A^{1/3} - \sqrt{3} - 1) > 0 \end{aligned}$$

for $A \in (0,1) \cup (10 + 6\sqrt{3}, \infty)$. Now, we have negative values for $\frac{B}{A}$ satisfying $\max\{-\frac{2}{\sqrt{A}}, -\frac{2}{A}\} < \frac{B}{A} < \min\{0, 1 - \frac{3}{A^{1/3}}\}$. On the other hand, it follows from (37) that $\mathrm{Eq}(\frac{1}{2}, \frac{1}{2}) = -\frac{1}{2}$ is the minimal value of $\mathrm{Eq}(X_{2a}, X_{2b})$. Thus, the negative values that $\mathrm{Eq}(X_{2a}, X_{2b})$ can reach belongs to $(-\frac{1}{2}, 0)$, which imposes an additional condition on A : $A \geq 4$. In summary, for this case there exist two Hopf critical points when $A > 10 + 6\sqrt{3}$ and $-2 < B < B_H^0$.

Further, it is noted that when $B \geq -2$, there is only one stable equilibrium E_1 for $0 < C \leq C_t$, which is located on the boundary of the trapping region. Thus, E_1 is globally asymptotically stable for $\max\{-2\sqrt{A}, -2\} < B < 0$ and $0 < C \leq C_t$. Combining the above results with that obtained for the case $B \geq 0$, we have proved part (a) of Theorem 6.

Next, consider the remaining case $-2\sqrt{A} < B < -2$, $(A > 1)$. As shown in Fig. 2(d), the upper branch E_2^- exists for $-\frac{2}{B} < X_2^- \leq 1$, which yields $BX_2^- + 2 < 0$, leading to $\det(J_2) < 0$. Thus, every point on the equilibrium E_2^- is a saddle. For the lower branch E_2^+, $0 < X_2^+ < -\frac{2}{B}$, and thus $BX_2^+ + 2 > 0$, yielding $\det(J_2) > 0$. Hence, similar to the above discussed cases, we can determine the stability of the equilibrium E_2^+ by using $\mathrm{Tr}(J_2)$ given in (32): E_2^+ is at least stable for $C \in (C_2, \infty)$, where C_2 is a positive constant because of $\mathrm{Tr}(J_2)|_{X_2=0} = -1$. Since one real solution of the equation $\mathrm{Tr}(J_2) = 0$ is negative, there are at most two positive Hopf critical points which can exist on E_2^+. However, for this case, the possibility of Hopf bifurcations is slightly different from the cases discussed above because single Hopf bifurcation is possible here due to that at $C = C^*$, $\mathrm{Tr}(J_2)$ can be positive and one positive solution appears on E_2^- at which the two real eigenvalues have the same absolute value but with opposite signs. In the following, we derive the conditions for the existence of Hopf bifurcations arising from the equilibrium E_2^+. One of the cases with two Hopf bifurcations is depicted in Fig. 2(d).

We still use the same formulas given in (29), (36) and (37) as well as the condition Disc given in (33) to consider various possibilities. First, note that now Disc < 0 does not guarantee the existence of two Hopf bifurcations, since the two positive roots may both lie on E_2^-, leading to no Hopf bifurcation; or one on E_2^- and the other on E_2^+, giving rise to one Hopf bifurcation; only when both are on E_2^+, then can we have two Hopf bifurcations. Thus, we need more conditions to classify the existence of Hopf bifurcations. It is easy to show that at the vertex $(C, X_2) = (C^*, -\frac{2}{B})$, $\det(J_2) = 0$ and $\mathrm{Tr}(J_2) = 1 + \frac{4}{B}$. Thus, we have

$$\mathrm{Tr}(J_2)|_{C=C^*} = 1 + \frac{4}{B} \begin{cases} < 0 & \text{if } \max\{-2\sqrt{A}, -4\} < B < -2, \\ & \qquad A > 1, \\ \geq 0 & \text{if } -2\sqrt{A} < B \leq -4, \quad A > 4. \end{cases} \tag{38}$$

Note that $B = -4$ is a critical case for which $\mathrm{Tr}(J_2) = 0$ at the turning point $(C, X_2) = (C^*, -\frac{2}{B})$, where a double zero eigenvalue is obtained, leading to a B–T bifurcation from the equilibrium E_2^+. Due to $\lim_{C\to+\infty} \mathrm{Tr}(J_2) = -1$, we know that when $\mathrm{Tr}(J_2)|_{C=C^*} \geq 0$, there must exist a Hopf bifurcation from E_2^+ (which coincides with the turning point if $B = -4$); while when $\mathrm{Tr}(J_2)|_{C=C^*} < 0$, there may exist none or two Hopf bifurcations from E_2^+. We first consider two Hopf bifurcations. Combining the above condition with Disc < 0 yields

$$A > 1 \quad \text{and} \quad \max\{-2\sqrt{A}, -4\} < B < B_H^{-2}.$$

The discussions in the above have shown that $B_H > -2\sqrt{A}$ for $A > 1$. We can also show that $B_H > -4$ for $A > 1$, $A \neq 2$. Then, to have two Hopf bifurcations, similar to the proof for Case (i), we need two solutions $0 < X_{2a}, X_{2b} < \frac{1}{2}$, such that $\mathrm{Eq}(X_{2a}, X_{2b})$ can have negative values in $(-\frac{1}{2}, 0)$. On the other hand, $\max\{-\frac{2}{\sqrt{A}}, -\frac{4}{A}\} < \frac{B}{A} < \min\{-\frac{2}{A}, \frac{B_H}{A}\}$, which requires $-\frac{2}{\sqrt{A}} > -\frac{1}{2}$ and $-\frac{4}{A} > -\frac{1}{2}$, leading to $A > 8$. Hence, when

$$A > 8 \quad \text{and} \quad -4 < B < B_H^{-2}, \tag{39}$$

the system has two Hopf bifurcations emerging from the equilibrium E_2^+.

Now we turn to one Hopf bifurcation. We have the conditions $A > 4$ and $-2\sqrt{A} < B \leq -4$. In addition, we need Disc ≤ 0, i.e. $B \leq B_H$. Hence, we obtain the conditions: $A > 4$ and $-2\sqrt{A} < B \leq B_H^{-4}$. However, we have shown that $B_H > -2\sqrt{A}$ for $A > 1$. Further, since $B_H + 4 = (A^{1/3} + 1)(A^{1/3} - 2)^2 > 0$ for $A \neq 8$. So the above condition can be rewritten as

$$A > 4 \quad \text{and} \quad -2\sqrt{A} < B < -4, \quad \text{or}$$
$$A > 4 \quad \text{and} \quad B = -4$$

and thus $-\frac{2}{\sqrt{A}} \leq \frac{B}{A} \leq -\frac{4}{A}$. For the first condition, $B < -4 \leq B_H$, indicating that Disc < 0. Thus, one of the positive solutions must be on E_2^-. Since $BX_2 + 2 < 0$ on E_2^-, (36) implies that the equation $\mathrm{Tr}(J_2) = 0$ can have solution $X_2 > \frac{1}{2}$. Thus, we may assume the two solutions satisfy $0 < X_{2a} < \frac{1}{2} < X_{2b} < 1$. Consequently, the minimal value that $\mathrm{Eq}(X_{2a}, X_{2b})$ can reach is $\mathrm{Eq}(\frac{1}{2}, 1) = -\frac{4}{3}$, leading to $\frac{-2}{\sqrt{A}} \geq -\frac{4}{3}$, i.e. $A \geq \frac{9}{4}$, which is satisfied under $A > 4$. Next, for $B = -4$, the equation $\mathrm{Tr}(J_2) = 0$ gives

$$\begin{aligned} &2AX_2^3 - (A+4)X_2^2 + 1 \\ &\quad = \frac{1}{A}(AX_2 + \sqrt{1+A} - 1)(2X_2 - 1) \\ &\qquad \times (AX_2 - \sqrt{1+A} - 1), \end{aligned}$$

showing that the trace $\mathrm{Tr}(J_2)$ always has a root at the turning point $X_{2a} = \frac{1}{2}$, and the second root is

$$X_{2b} = \frac{\sqrt{1+A}+1}{A} \begin{cases} > \frac{1}{2}, & \text{if } 4 < A < 8, \\ = \frac{1}{2}, & \text{if } A = 8, \\ < \frac{1}{2}, & \text{if } A > 8. \end{cases}$$

This indicates that when $B = -4$, $4 < A \leq 8$, there is no Hopf bifurcation to occur on E_2^+ except the turning point $X_2 = \frac{1}{2}$. Summarizing the above discussions we have that if

$$\begin{gathered} A > 4 \quad \text{and} \quad -2\sqrt{A} < B < -4, \quad \text{or} \\ A > 8 \quad \text{and} \quad B = -4, \end{gathered} \tag{40}$$

the system $\mathrm{A_{iii}}$ has one Hopf bifurcation arising from E_2^+. When both (39) and (40) are not satisfied, there is no Hopf bifurcation.

To this end, the remaining question for Case (ii) when $-2\sqrt{A} < B < -2$, $(A > 1)$ is whether the lower branch E_2^+ can have Hopf bifurcation in the interval $C \in (C^*, C_t)$. If this can happen, then the equilibrium solutions E_1 and E_2 coexist for $C \in (C^*, C_t)$ and both of them are stable, leading to the so-called bistable phenomenon. It is more interesting to see another type of bistable phenomenon which involves stable equilibria and stable periodic motions. If we can find parameter values such that $\mathrm{Tr}(J_2)|_{C=C^*}\mathrm{Tr}(J_2)|_{C=C_t} < 0$, then we can conclude that there exist one Hopf bifurcation in the interval $C \in (C^*, C_t)$. If $\mathrm{Tr}(J_2)|_{C=C^*}\mathrm{Tr}(J_2)|_{C=C_t} > 0$, then in the interval $C \in (C^*, C_t)$, there are either no Hopf bifurcations or two Hopf bifurcations. Therefore, when at least one Hopf critical point is located in this interval, $C_H \in (C^*, C_t)$, bistable phenomenon involving an equilibrium and stable limit cycles is possible to exist. It should be noted that a saddle-node bifurcation occurs at the vertex $(C, X_2) = (C^*, -\frac{2}{B})$, and when the parameters are varied such that the equilibrium solution moves from E_2^- to E_2^+ through the vertex, the equilibrium E_2^+ may be stable or unstable depending upon the sign $\mathrm{Tr}(J_2)|_{C=C^*}$.

Note that at $C = C_t$, the equation $F_1 = 0$ has two solutions $X_2 = 1$ and $X_2 = -\frac{1}{1+B}$. So, in order to determine the sign of $\mathrm{Tr}(J_2)|_{C=C_t}$, we substitute the second solution into $\mathrm{Tr}(J_2)$ to obtain

$$\mathrm{Tr}(J_2)|_{C=C_t} = \frac{1}{(1+B)(A+B+1)}[A(B+3) - (B+1)(B^2+3B+1)]. \tag{41}$$

Since $A+B+1 > 0$ and $1+B < 0$, $\mathrm{Tr}(J_2)|_{C=C_t}$ can be positive or negative depending upon the parameter values of A and B. More precisely, we have

$$\mathrm{Tr}(J_2)|_{C=C_t} < 0 \quad \text{for} \begin{cases} \dfrac{9}{4} < A < A_H, & \text{if } -2\sqrt{A} < B < -3, \\ A > \dfrac{9}{4}, & \text{if } B = -3, \\ A > \dfrac{7+3\sqrt{5}}{8}, & \text{if } \max\{-2\sqrt{A}, -3\} < B \le -\dfrac{3+\sqrt{5}}{2}, \\ A > 1, & \text{if } \max\left\{-2\sqrt{A}, -\dfrac{3+\sqrt{5}}{2}\right\} < B < -2, \end{cases}$$

$$\mathrm{Tr}(J_2)|_{C=C_t} > 0, \quad \text{otherwise.}$$

Now combining the above conditions with that for one Hopf bifurcation obtained above, we have that one Hopf bifurcation exists with $C_H \in (C^*, C_t)$ if $4 < A < A_H$ when $-2\sqrt{A} < B < -4$; or if $A > A_H$ when $-4 < B < B_H^{-3}$. For the case of two Hopf bifurcations, it is more complicated since the restriction on $X_2 \in (0, \frac{1}{2})$ and the condition given in (39) are not enough. Note that now $-\frac{1}{1+B} < X_2 < -\frac{1}{2}$, which yields $B < -3$. With this condition, combining the conditions given in (39) and $\mathrm{Tr}(J_2)|_{C=C_t} < 0$ we obtain two Hopf bifurcations appearing on E_2^+ satisfying $C^* < C_{H_1} < C_{H_2} < C_t$ if $8 < A < A_H$ when $-4 < B < B_H^{-3}$.

The bifurcation diagrams for Case (ii) are shown in Figs. 2(b)–2(d), corresponding to cases when B takes different values from the intervals $B < -2$, $-2 < B < -1$ and $-1 < B < 0$, respectively, together with the condition $B > -2\sqrt{A}$. Here, C^* and C_t are defined in (26) and (28), respectively, and C_{H_1} and C_{H_2} denote two Hopf critical points. Note that the vertex moves down when B is decreasing, and the points $C = C_t$ and $C = AD$ exchange their relative positions when B crosses the value $B = -1$. The bistable equilibrium solutions E_1 and E_2^+ are marked by blue and green colors, respectively.

Finally, we consider stability of bifurcating limit cycles from E_2^+, which requires computing the focus values of the system. For convenience, let

$$C = C_t + E, \quad \text{if } B > \max\{-2\sqrt{A}, -2\},$$
$$C = C^* + E, \quad \text{if } -2\sqrt{A} < B \le -2 \ (A > 1),$$

where $E > 0$. Further, we use the parameters A and E to solve the equilibrium solution and the critical stability condition $\mathrm{Tr}(J_2) = 0$, yielding

$$A = \frac{BX_2^2 + 1}{X_2^2(1-2X_2)},$$
$$E = \begin{cases} \dfrac{D(1-X_2)(BX_2+X_2+1)}{X_2^2}, \\ \qquad \text{if } B > \max\{-2\sqrt{A}, -2\}, \\ \dfrac{D(BX_2+2)^2}{4X_2^2}, \\ \qquad \text{if } -2\sqrt{A} < B \le -2 \ (A > 1), \end{cases} \tag{42}$$

which indicates that $A > 0$ and $E > 0$, as expected, since $0 < X_2 < \frac{1}{2}$. Moreover, at these values, we have

$$\omega_c = (BX_2+2)(1-X_2)\sqrt{\frac{D}{1-2X_2}}$$
$$> 0, \quad \forall\, X_2 \in \left(0, \frac{1}{2}\right). \tag{43}$$

Further, we introduce an additional time scaling $\tau = (AX^2 + BX + 1)\tau_1$ and a linear transformation into system A_{iii} to obtain a system with its linear part in Jordan canonical form. Then, executing our Maple program [Yu, 1998] on the resulting system yields the first-order focus value:

$$v_1 = -\frac{\overline{v}_1}{8X_2(1-2X_2)(BX_2+2)}, \quad \text{where}$$

$$\overline{v}_1 = B + 2B^2X_2^3 + 6BX_2^2 + 6. \tag{44}$$

It is easy to see that $\overline{v}_1 > 0$ when $B \geq 0$ and $X_2 \in (0, \frac{1}{2})$. When $B > -2$, $\overline{v}_1 = B + 2 + 2(B^2X_2^3 + 2 + 3BX_2^2) > 0$ since $3BX_2^2 > -\frac{3}{2}$ for $X_2 \in (0, \frac{1}{2})$.

When $-2\sqrt{A} < B \leq -2$ $(A > 1)$, we rewrite $\overline{v}_1$ as

$$\overline{v}_1 = 8\left(\frac{1}{2} - X_2\right)^2 (1 + 4X_2) + (B+4)v_1^*, \quad \text{where}$$

$$v_1^* = 1 + 2(B-4)X_2^3 + 6X_2^2.$$

First consider two Hopf bifurcations for which $B > -4$, and the two Hopf critical points are located in the interval $X_2 \in (0, \frac{1}{2})$. In addition, it is easy to show that $v_1^* > 1 - 16X_2^3 + 6X_2^2$ which reaches its minimum $\frac{1}{2}$ for $X_2 \in [0, \frac{1}{2}]$. Therefore, $v_1^* > 0$, leading to $\overline{v}_1 > 0$ and so $v_1 < 0$, implying that both of the two Hopf bifurcations are supercritical and the bifurcating limit cycles are stable.

Next, consider one Hopf bifurcation. The case $A > 8$, $B = -4$ is straightforward since $\overline{v}_1 > 0$ and thus the Hopf bifurcation is supercritical. For the case $A > 4$, $-2\sqrt{A} < B < -4$, first note that when $B \leq -6$, we can rewrite $\overline{v}_1$ to obtain $\overline{v}_1 = 6BX_2^2(1 + \frac{BX_2}{3}) + B + 6 < 0$ since $1 + \frac{BX_2}{3} \geq 1 - \frac{2}{3} = \frac{1}{3}$ due to $X_2 \leq \frac{-2}{B}$, which gives $v_1 > 0$ and so the Hopf bifurcation is subcritical and bifurcating limit cycles are unstable. For $-6 < B < -4$, $\overline{v}_1$ may take negative or positive values. The condition for $\overline{v}_1 = 0$ can be found from eliminating X_2 from the equations $\mathrm{Tr}(J_2) = 0$ and $\overline{v}_1 = 0$ as $A = \frac{B^2}{6+B}$. Then, for $-6 < B < -4$, we have

$$v_1 \begin{cases} = 0, & \text{for } X_2 = X_2^* \in \left(0, \dfrac{-2}{B}\right), \text{ if } A = \dfrac{B^2}{6+B}, \\ < 0, & \text{for } 0 < X_2 < X_2^* < \dfrac{-2}{B}, \text{ if } A > \dfrac{B^2}{6+B}, \\ > 0, & \text{for } 0 < X_2^* < X_2 < \dfrac{-2}{B}, \text{ if } A < \dfrac{B^2}{6+B}. \end{cases}$$

In summary, we conclude that except when $A > 9$, $B \leq -6$ and $A < \frac{B^2}{B+6}$, $-6 < B < -4$, the single Hopf bifurcation from E_2^+ is subcritical and bifurcating limit cycles are unstable, all other Hopf bifurcations including two Hopf bifurcations and single Hopf bifurcation are supercritical and bifurcating limit cycles are stable. The critical case $v_1 = 0$ yields generalized Hopf bifurcation, leading to bifurcation of multiple limit cycles, and will be considered in the next subsection.

This completes the proof for Theorem 6. ■

3.3.3. *Two limit cycles from generalized Hopf bifurcation*

In the previous subsection, we have identified the conditions on the parameters under which the first-order focus value v_1 vanishes. This implies that it is possible for the system A_{iii} to have multiple limit cycles bifurcating from a Hopf critical point. We have the following theorem.

Theorem 7. *For system* A_{iii}, *generalized Hopf bifurcation can occur from* E_2^+ *when* $A = \frac{B^2}{B+6}$, $C = \frac{D(2+BX_2)(1-X_2)}{X_2^2(1-2X_2)}$ *and* $B \in (-6, -4)$, $X_2 \in (0, \frac{-2}{B})$, *yielding maximal two limit cycles bifurcating from a Hopf critical point. Moreover, when* $v_1 = 0$, $v_2 < 0$, *implying that the outer of the two bifurcating limit cycles is stable while the inner one is unstable, and both limit cycles enclose the stable focus* E_2^+.

Proof. We first solve $F_1 = 0$ for C, and then solve $\mathrm{Tr}(J_2) = 0$ for A to obtain

$$A = \frac{1 + BX_2^2}{X_2^2(1-2X_2)},$$

$$C = \frac{D}{X_2^2}(AX_2^2 + BX_2 + 1)$$

$$= \frac{D(2+BX_2)(1-X_2)}{X_2^2(1-2X_2)},$$

$$\text{with } B \in (-6, -4) \quad \text{and} \quad X_2 \in \left(0, \frac{-2}{B}\right). \tag{45}$$

Since $0 < X_2 < \frac{-2}{B}$, we have $2 + BX_2 > 0$, and thus $0 < X_2 < \frac{1}{2}$, yielding $C > 0$, which in turn results in $1 + BX_2^2 > 0$, and so $A > 0$. With the above conditions, we execute our Maple program for computing Hopf and generalized Hopf bifurcations to

get v_1 given in (44) and

$$\begin{aligned} v_2 = {} & \frac{1}{192DX_2^3(1-X_2)^2(1-2X_2)^2(2+BX_2)^3}\{\overline{v}_1[76(1-3X_2-BX_2^3)^2+3D^2(1-2X_2)^2(2+BX_2)^2] \\ & + D(2X_2-1)[4B^4X_2^7+4B^3(27B-37)X_2^6-2B^2(27B^2-521B+442)X_2^5 \\ & - 2B(237B^2-1681B+582)X_2^4+2B(19B^2-659B+1454)X_2^3 \\ & - (1164+23B^3-233B^2-424B)X_2^2-(175B^2+392B-3372)X_2-4(67B+378)]\}, \end{aligned} \tag{46}$$

where $\overline{v}_1$ is given in (44). Now, setting $v_1 = 0$ (i.e. $\overline{v}_1 = 0$) we obtain $A = \frac{B^2}{B+6}$, as expected. We have shown in the previous subsection that $\tilde{v}_1 = 0$ has real solutions under the conditions given in (45), for which we have

$$\begin{aligned} v_2|_{v_1=0} = {} & -\frac{1}{192X_2^3(1-X_2)^2(1-2X_2)(2+BX_2)^3}[4B^4X_2^7+4B^3(27B-37)X_2^6 \\ & - 2B^2(27B^2-521B+442)X_2^5-2B(237B^2-1681B+582)X_2^4 \\ & + 2B(19B^2-659B+1454)X_2^3-(1164+23B^3-233B^2-424B)X_2^2 \\ & - (175B^2+392B-3372)X_2-4(67B+378)]. \end{aligned}$$

Further, we use the Groebner basis reduction procedure to reduce the above expressions to obtain when $v_1 = 0$,

$$\begin{aligned} v_2 = {} & -\frac{1}{96X_2^3(1-X_2)^2(1-2X_2)(2+BX_2)^3}\tilde{v}_2, \quad \text{where} \\ \tilde{v}_2 = {} & 24BX_2^4-100BX_2^3+2(B^3+21B^2+83B+12)X_2^2 \\ & - 3(3B^2+8B+36)X_2+4B^2+45B+174. \end{aligned} \tag{47}$$

In the following, we show that $v_2 < 0$ when $\overline{v}_1 = 0$. To achieve this, first we solve $\overline{v}_1 = 0$ for B to obtain

$$B_\pm = \frac{1}{4X_2^3}[-(1+6X_2^2) \pm \sqrt{(1+6X_2^2)^2-48X_2^3}].$$

It can be shown that B_- is not a solution satisfying $B \in (-6,-4)$, and B_+ is a solution. We can rewrite B_+ as

$$B_+ = \frac{1}{4X_2^3}\{-(1+6X_2^2)+\sqrt{4X_2^4+(1-2X_2)[1+2X_2+16X_2^2(1-X_2)]}\},$$

indicating that the term in the square root is positive for $X_2 \in (0, \frac{1}{2})$. Now substituting B_+ into v_2 we obtain

$$\begin{aligned} v_2 = {} & -\frac{1}{768X_2^{10}(1-2X_2)(2+BX_2)^3}\{[48X_2^6+(1-2X_2)(1+52X_2^4+4X_2^2(4-3X_2))] \\ & \times\sqrt{4X_2^4+(1-2X_2)[1+2X_2+16X_2^2(1-X_2)]}-[96X_2^8+(1-2X_2)(1+16X_2^5+312X_2^6 \\ & + 2X_2^2(1-2X_2)(24X_2^4+82X_2^2+4X_2+11))]\}. \end{aligned}$$

Proving $v_2 < 0$ is equivalent to proving that the term in the script bracket of v_2 is positive. It is easy to see that the two terms in the two square brackets are positive, thus it suffices to prove that

$$\begin{aligned} & [48X_2^6+(1-2X_2)(1+52X_2^4+4X_2^2(4-3X_2))]^2\{4X_2^4+(1-2X_2)[1+2X_2+16X_2^2(1-X_2)]\} \\ & \quad - \{96X_2^8+(1-2X_2)[1+16X_2^5+312X_2^6+2X_2^2(1-2X_2)(24X_2^4+82X_2^2+4X_2+11)]\}^2 \\ & \quad = 768X_2^7(1+2X_2+12X_2^2)(1-X_2)^2(1-2X_2)^3 > 0, \end{aligned}$$

which is true for $X_2 \in (0, \frac{1}{2})$ provided that the conditions in (45) and $v_1 = 0$ hold.

The above result shows that for any parameter values satisfying (45), the outer of the two bifurcating limit cycles is always stable while the inner one is unstable, and both limit cycles enclose the stable focus E_2^+. ■

Remark 3.2. It is seen from (45) that this generalized Hopf bifurcation belongs to the case $B \in (-2\sqrt{A}, -2)$ $(A > 1)$, see Fig. 2(d). Moreover, it follows from the proof for Case (ii) of Theorem 5 that this case corresponds to single Hopf bifurcation because

$$\begin{aligned} A - 4 &= \frac{B^2}{B+6} - 4 \\ &= \frac{B^2 - 4B - 24}{B+6} \\ &= \frac{(B+6)^2 - 16(B+4) + 4}{B+6} > 0. \end{aligned}$$

Further, the proof for Case (ii) of Theorem 5 tells us that the Hopf critical point C_H can occur in the interval (C^*, C_t) if $4 < A < A_H$, which generates more complex dynamical behaviors such as tristable phenomenon. The following calculation shows that

$$\begin{aligned} A - A_H &= \frac{B^2}{B+6} - B(B+1) - \frac{B+1}{B+3} \\ &= -\frac{B+2}{(B+3)(B+6)}(B^3 + 7B^2 + 11B + 3) \\ &\Rightarrow A < A_H \Leftrightarrow B^3 + 7B^2 + 11B + 3 > 0 \\ &\qquad \forall\, B \in (-6, -4). \end{aligned}$$

It is not difficult to verify that

$$B^3 + 7B^2 + 11B + 3 \begin{cases} > 0 & \text{for } B \in (-4.8661, -4), \\ < 0 & \text{for } B \in (-6, -4.8661). \end{cases}$$

Therefore, if $B \in (-6, -4.8661)$, then $C_H > C_t$, and stable equilibria E_1 and E_2^+ coexist for $C \in (C^*, C_t)$; while stable equilibrium E_2^+ and stable limit cycle coexist near C_H, and an unstable limit cycle exists between E_2^+ and the stable limit cycle. When $B \in (-4.8661, -4)$, $C_H \in (C^*, C_t)$, and stable equilibria E_1 and E_2^+ coexist for $C \in (C_H, C_t)$; while the two stable equilibria and two limit cycles coexist for $C \in (C^*, C_H)$, yielding tristable phenomenon, that is, two stable equilibria and one stable limit cycle coexist with an unstable limit cycle between E_2^+ and the stable limit cycle.

To end this subsection, we present two numerical examples to illustrate the result of Theorem 7. We choose $B = -5$ and $B = -4.5$ for the two examples. First, consider $B = -5$ for which we have $A = 25$. Then solving $v_1 = 0$ we obtain $X_2 = 0.233650\ldots$, for which $v_1 = 0$ and $v_2 = -22.342154\ldots < 0$, as expected. For these parameter values, $C_H = 21.918007\ldots D$, where D is free to choose, which can be used to adjust the parameter values. This indeed shows that $C_H > C_t = (A + B + 1)D = 21D$. We choose $D = 0.05$ and so $C_H \approx 1.0959$. Then, we give perturbations to A and B as $B = -5 - 0.01$ and $A = \frac{B^2}{B+6} - 0.37245$, for which $v_0\mu \approx -0.600273 \times 10^{-6}$, $v_1 = 0.012983$ and $v_2 \approx -32.852477$. Thus, the truncated normal form equation,

$$\begin{aligned} \dot{r} &= r(v_0\mu + v_1 r^2 + v_2 r^4) \\ &= r(-0.600273 \times 10^{-6} + 0.012983 r^2 \\ &\quad - 32.852477 r^4), \end{aligned}$$

gives the approximate solutions for the amplitudes of the two limit cycles: $r_1 \approx 0.0073$ and $r_2 \approx 0.0185$.

Next, for $B = -\frac{9}{2}$, we have $A = \frac{27}{2}$, and then solve $v_1 = 0$ to obtain $X_2 = \frac{1}{3}$, for which $v_1 = 0$ and $v_2 = -\frac{243}{16}$. In addition, we have $C_H = 9D \in (C^*, C_t) = (\frac{135}{16}D, 10D)$. Again we choose $D = \frac{1}{20}$, and so $C_H = \frac{9}{20}$, $C^* = \frac{27}{64}$ and $C_t = \frac{1}{2}$. Further, we give perturbations to A and B as $B = -\frac{9}{2} - \frac{1}{100}$ and $A = \frac{B^2}{B+6} - 0.18112$, and then obtain $v_0\mu \approx -0.855083 \times 10^{-6}$, $v_1 \approx 0.022634$ and $v_2 \approx -26.766197$. Thus, we have the truncated normal form equation,

$$\begin{aligned} \dot{r} = r(&-0.855083 \times 10^{-6} \\ &+ 0.022634 r^2 - 26.766197 r^4), \end{aligned}$$

which yields the approximations for the amplitudes of the two limit cycles: $r_1 \approx 0.0063$ and $r_2 \approx 0.0284$.

Simulation for the second example to yield the tristable phenomenon is given in the next section.

4. Simulations

In this section, we present simulations to demonstrate the dynamics and bifurcations predicted using the analytical method in the previous sections. We show the simulations for A_i without limit cycles, and for A_{iii} with one limit cycle and two limit cycles. All the simulation results are obtained by

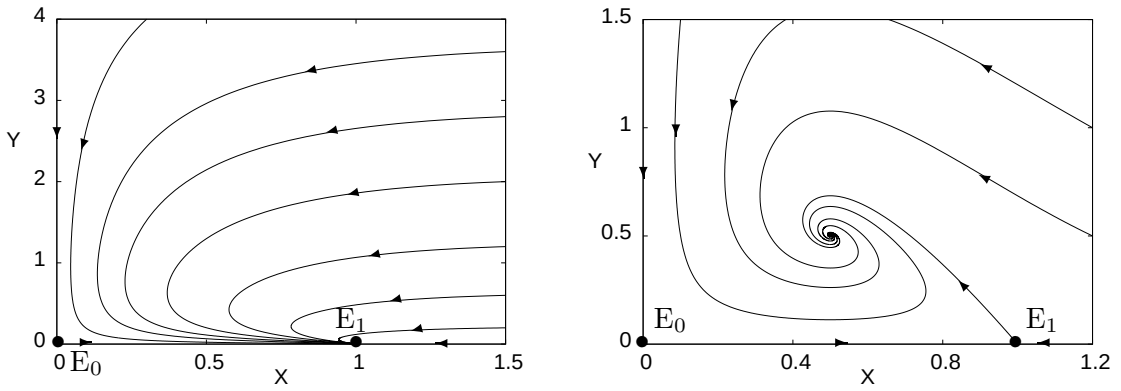

(a) (b)

Fig. 4. Simulated phase portrait for system A_i with $D = 1$ showing (a) convergence to the equilibrium $E_1 : (1, 0)$ for $C = 0.5$ and (b) convergence to the equilibrium $E_2 : (0.5, 0.5)$ for $C = 2$.

using a fourth-order Runge–Kutta numerical integration method on a PC machine.

4.1. A_i — *No limit cycle*

For this system, we have shown that the equilibrium $E_0 : (0, 0)$ is a saddle point, the equilibrium $E_1 : (1, 0)$ is a node, globally asymptotically stable for $C \le D$, and the positive equilibrium E_2 exists and is globally asymptotically stable for $C > D$. We take $D = 1$. The simulation for $C = 0.5$ is depicted in Fig. 4(a), showing that all trajectories converge to E_1; and the simulation for $C = 2$, as shown in Fig. 4(b), indeed demonstrates that all trajectories converge to $E_2 : (0.5, 0.5)$. No Hopf bifurcation occurs, nor can any types of periodic motions exist.

4.2. A_{iii} — *One limit cycle*

For system A_{iii}, it has been shown that when $X_2 \in (0, 1)$ (implying that $C > C_t = (A+B+1)D$) and $B > \max\{-2\sqrt{A}, -2\}$, $\det(J_2) > 0$. Thus, in this case the stability of E_2 is determined by $\mathrm{Tr}(J_2)$. We first consider $B \ge 0$, and, for example, take $A = B = D = 1$. It follows from the proof for Case (i) of Theorem 6 that E_2 is always stable. In fact, when $A = B = D = 1$, we have

$$\mathrm{Tr}(J_2) = -\frac{2[2C^3(C-3) + 2C(9C-5) + (C^3 - C^2 + 5C - 3)(\sqrt{4C-3} - 1)]}{C(C-1)(2C - 1 + \sqrt{4C-3})^2} < 0$$

for $C > C_t = 3$.

In order to have Hopf bifurcation from E_2^+, we choose $D = 1$, $A = 36 > 27$, $B = 3 < B_H \approx 3.2918$, which yields two critical Hopf bifurcation points: $C_{H_1} = 54$ and $C_{H_2} = 60$. Therefore, the equilibrium E_1 is globally asymptotically stable for $0 < C < C_t = 40$, while the equilibrium E_2^+ exists for $C > 40$ and is asymptotically stable for $C \in (40, 54) \cup (60, \infty)$, but unstable for $54 < C < 60$. The simulations for $C = 30, 48, 70$ and 57 are shown in Figs. 5(a)–5(d), respectively. It is seen from these figures that simulations agree with the analytical predictions: all trajectories converge to the stable node $E_1 : (1, 0)$ when $C = 30$; and converge to the stable node E_2^+ when $C = 48$ and 70; but converge to a stable limit cycle enclosing the equilibrium E_2^+ when $C = 57$. In fact, for any values of $C \in (54, 60)$, the system exhibits a stable limit cycle due to Hopf bifurcation, agreeing with Theorem 6.

Next, we consider the case for $-2\sqrt{A} < B \le -2$, $(A > 1)$. In order to illustrate the results of Theorem 6, we fix $D = 1$ and give a number of numerical examples with different values of A, B and C to show different types of bifurcations and stability. The results are listed in Table 2. We choose $B = -3.5$, $A = 15$ (see the sixth column in Table 2, and take six values of $C : 10, 12, 12.35, 12.5, 14$ and 16, satisfying $10 < C^* < 12 < C_{H_1} < 12.35 < C_t = 12.5 < C_{H_2} < 14 < 16$, to simulate the system A_{iii}, yielding the phase portraits as depicted in

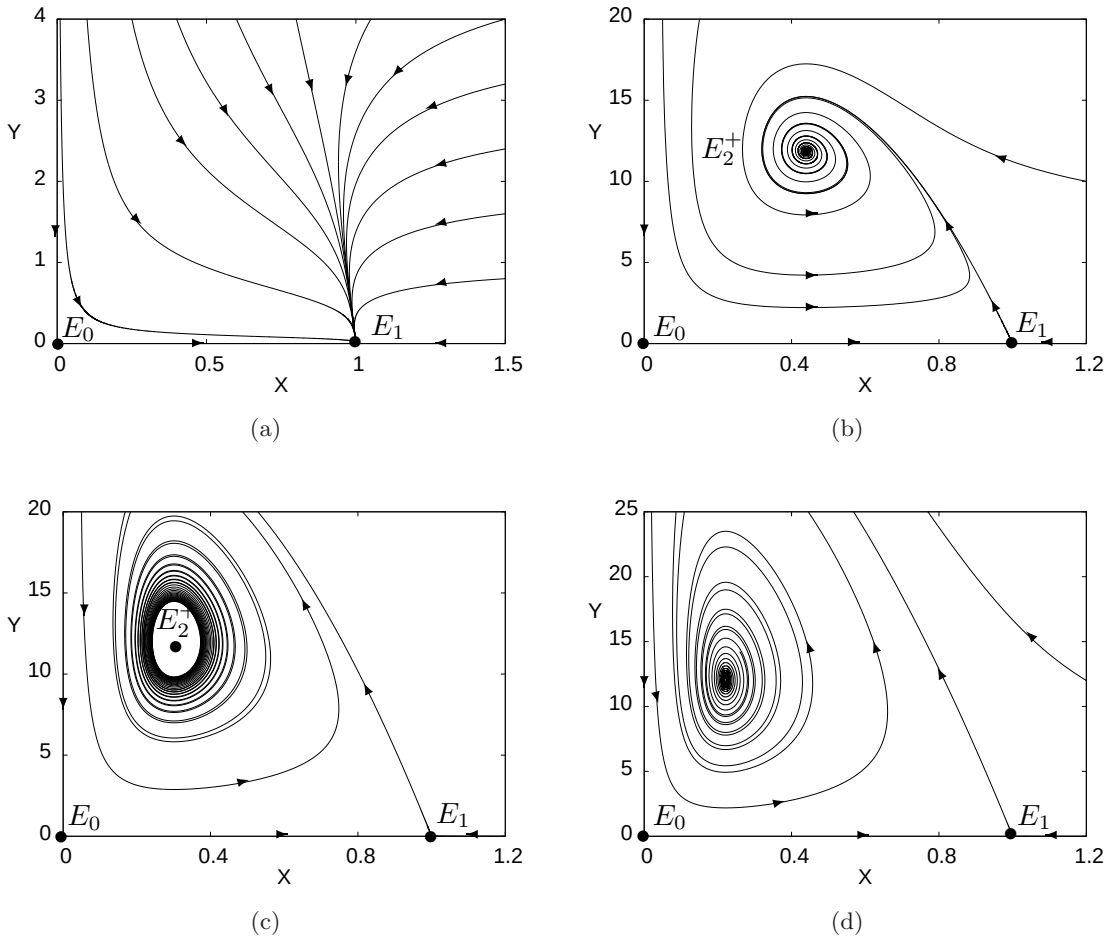

Fig. 5. Simulated phase portraits for system A_{iii} with $A = 36$, $B = 3$, $D = 1$, showing the convergence of the trajectories: (a) to $E_1 : (1, 0)$ when $C = 30$, (b) to $E_2^+ : (\frac{1}{24}(3 + \sqrt{57}), \frac{1}{2}(1 + 3\sqrt{57}))$ when $C = 48$, (c) to a stable limit cycle when $C = 57$ and (d) to $E_2^+ : (\frac{1}{68}(3 + \sqrt{145}), \frac{35}{1156}(25 + 31\sqrt{145}))$ when $C = 70$.

Figs. 6(a)–6(f), respectively. As predicted by the analytical results, we can see from these figures that all trajectories converge to the equilibrium E_1 when $C = 10$ [see Fig. 6(a)]; trajectories converge to either the equilibrium E_1 or the equilibrium E_2^+ depending on the initial conditions when $C = 12$ [see Fig. 6(b)]; trajectories converge either to the equilibrium E_1 or to a stable limit cycle enclosing E_2^+ depending on the initial conditions for $C = 12.35$ [see Fig. 6(c)]; converge to a stable limit cycle for $C = 12.5$ [see Fig. 6(d)]; and converge to the equilibrium E_2^+ when $C = 14, 16$ [see Figs. 6(e) and 6(f)]. Note that $C = 12.5 = C_t$ is a critical case for which the two equilibria E_1 and E_2^- coincide, yielding a degenerate saddle point.

4.3. A_{iii} — *Two limit cycles*

Finally, we give a simulation on the bifurcation of two limit cycles in system A_{iii}. We take the perturbed parameter values for the second numerical example considered in Sec. 3.3.3,

$$A = 13.4699538255, \quad B = -4.51, \quad C = 0.4469976913, \quad D = 0.05. \tag{48}$$

The simulation is given in Fig. 7, where two limit cycles are clearly shown in a zoomed region, see Fig. 7(b). The small unstable limit cycle is obtained by using the backward time steps (i.e. taking negative time steps so that the unstable limit cycle becomes "stable" in simulation). It can be seen from Fig. 7 that the amplitudes of the two simulated limit cycles are in a good agreement with the analytical predictions obtained in the previous section: $r_1 \approx 0.0063$ and $r_2 = 0.0284$.

This example shows an interesting tristable phenomenon, that is, depending upon initial conditions, solution trajectories may converge to the stable equilibrium $E_1 : (1, 0)$, or to the stable equilibrium $E_2^+ : (0.333333, 1.986656)$, or to the stable

Table 2. Different types of bifurcations and stability for system A_{iii}.

B	-3.5	-5	-5	-3.5	-3.5	-3
A	12.5	20	35	13.6	15	20
C^*	9.43755	13.75	28.75	10.5375	11.9375	17.75
C_t	10	16	31	11.1	12.5	18
$\mathrm{Tr}(J_2(C^*))$	$-\frac{1}{7}$	$\frac{1}{5}$	$\frac{1}{5}$	-0.1429	$-\frac{1}{7}$	$-\frac{1}{3}$
$\mathrm{Tr}(J_2(C_t))$	$-\frac{1}{40}$	$-\frac{1}{8}$	$\frac{11}{62}$	-0.0027	$-\frac{1}{50}$	$-\frac{1}{18}$
Hopf	0	1	1	2	2	2
C_H or (C_{H_1}, C_{H_2})	—	15.4581	35.6931	10.8837 11.0084	12.1286 12.9739	18.2480 20.9762
1st focus value	—	0.2391	-0.2372	-1.9810 -2.3103	-1.5502 -3.6096	-1.7746 -4.5169
Bistable vs. C	$\mathrm{E}_1, \mathrm{E}_2^+$ (C^*, C_t)	$\mathrm{E}_1, \mathrm{E}_2^+$ (C_H, C_t)	$\mathrm{E}_1, \mathrm{LC}$ (C^*, C_t)	$\mathrm{E}_1, \mathrm{E}_2^+$ $(C^*, C_{H_1}) \cup (C_{H_2}, C_t)$ $\mathrm{E}_1, \mathrm{LC}$ (C_{H_1}, C_{H_2})	$\mathrm{E}_1, \mathrm{E}_2^+$ (C^*, C_{H_1}) $\mathrm{E}_1, \mathrm{LC}$ (C_{H_1}, C_t)	$\mathrm{E}_1, \mathrm{E}_2^+$ (C^*, C_t)

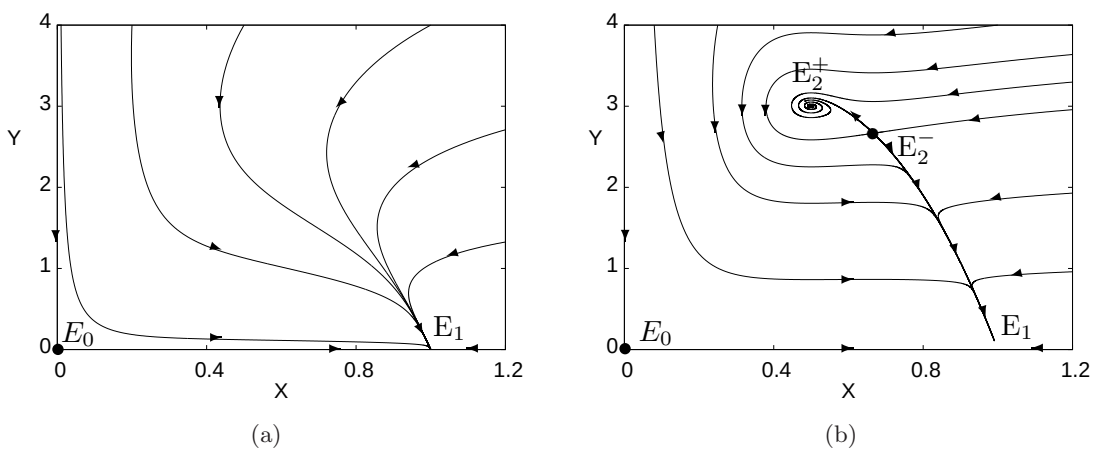

(a) (b)

Fig. 6. Simulated phase portraits for system A_{iii} with $A = 15$, $B = -3.5$, $D = 1$, showing the convergence of the trajectories to (a) $\mathrm{E}_1 : (1, 0)$ when $C = 10$, (b) either $\mathrm{E}_1 : (1, 0)$ or $\mathrm{E}_2^+ : (0.5, 3)$ when $C = 12$, (c) either $\mathrm{E}_1 : (1, 0)$ or a stable limit cycle when $C = 12.35$, (d) a stable limit cycle when $C = 12.5$, (e) E_2^+ when $C = 14$ and (f) E_2^+ when $C = 16$.

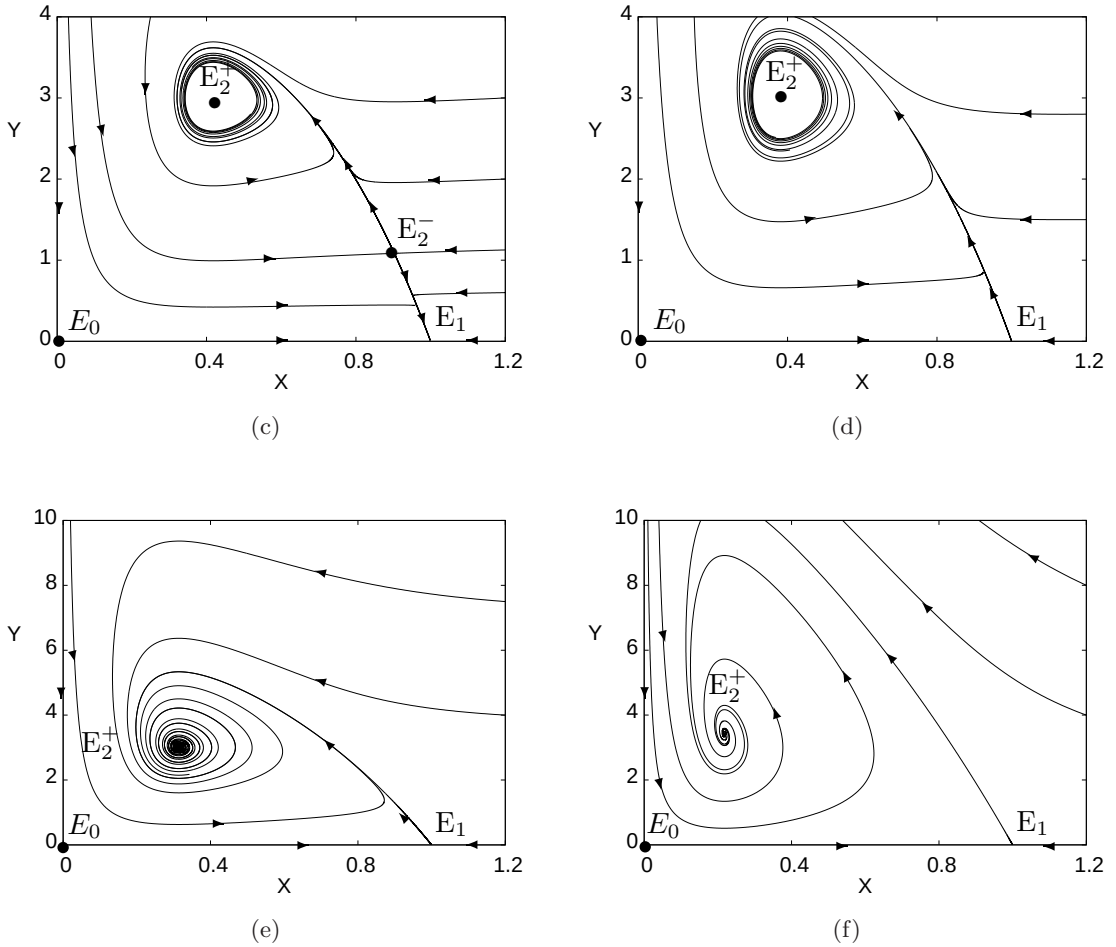

(c) (d)

(e) (f)

Fig. 6. (*Continued*)

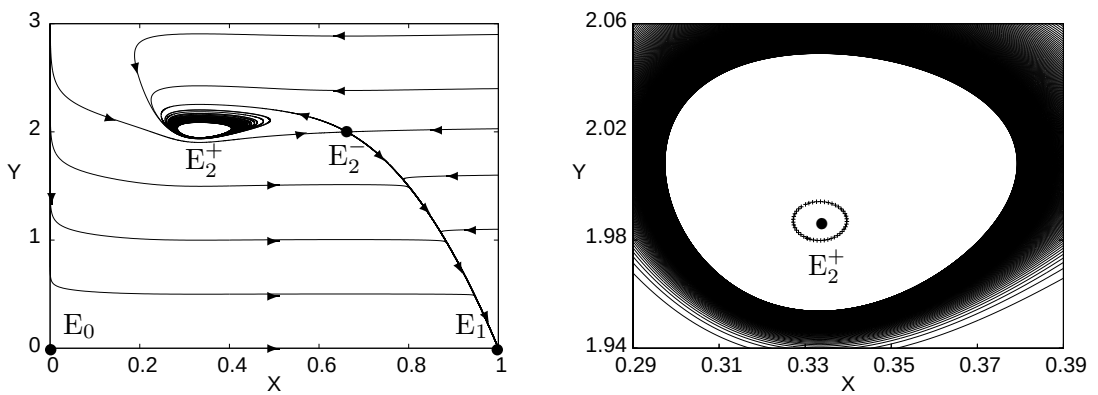

(a) (b)

Fig. 7. Simulated phase portraits for system A_{iii} with $A = 13.4699538255$, $B = -4.51$, $C = 0.4469976913$, $D = 0.05$ showing (a) tristable phenomenon, with trajectories converging to the stable equilibria $E_1 : (1, 0)$ and $E_2^+ : (0.333333, 1.986656)$, and to the stable limit cycle and (b) zoomed region to show the two limit cycles with outer stable and inner unstable equilibria.

limit cycle. The stable and unstable manifolds from the saddle E_2^- separate the trapping areas for the stable equilibrium E_1 and the stable limit cycle [the part outside the stable limit cycle, see Fig. 7(a)]; while the unstable limit cycle separates the trapping areas for the stable equilibrium E_1 and the stable limit cycle [the part inside the stable limit cycle, see Fig. 7(b)]. This indeed demonstrates a very complex dynamical behavior in predator–prey systems due to Hopf bifurcation, which may describe more realistic situations in these models.

5. Conclusion

In this paper, we have studied in detail five predator–prey systems with various Holling type functional responses. We have shown that under parameter variations, these systems can exhibit different bifurcations of limit cycles and complex dynamics. In particular, bistable and tristable phenomena can occur, leading to the coexistence of stable equilibria and stable limit cycles. This indicates that some complex dynamical behavior in biological systems may be generated by bifurcation of limit cycles. The dynamical study of systems (8)–(11) will be presented in forthcoming papers, showing bifurcation of even four limit cycles around a Hopf critical point. This will indeed demonstrate that predator–prey models can have very complex dynamical behaviors.

Acknowledgments

This research was partially supported by the National Natural Science Foundation of China (No. 11201294), the Innovation Program of Shanghai Municipal Education Commission (No. 14YZ114), and the Natural Science and Engineering Research Council of Canada (No. R2686A02).

References

Arditi, R. & Ginzburg, L. R. [1989] "Coupling in predator–prey dynamics: Ratio dependence," *J. Theor. Biol.* **139**, 311–326.

Bautin, N. [1952] "On the number of limit cycles appearing from an equilibrium point of the focus or center type under varying coefficients," *Matem. Sb.* **30**, 181–196.

Bazykin, A. D. [1998] *Nonlinear Dynamics of Interaction Populations*, World Sci. Ser. Nonlinear Sci. Ser. A., Vol. 11 (World Scientific, Singapore).

Carr, J. [1981] *Applications of Center Manifold Theory* (Springer, NY).

Chow, S. N. & Hale, J. K. [1982] *Methods of Bifurcation Theory* (Springer, NY).

Chow, S. N., Li, C. C. & Wang, D. [1994] *Normal Forms and Bifurcation of Planar Vector Fields* (Cambridge University Press, Cambridge).

Freedman, H. I. [1980] *Deterministic Mathematical Models in Population Ecology* (Marcel Dekker, NY).

Gazor, M. & Yu, P. [2012] "Spectral sequences and parametric normal forms," *J. Diff. Eqs.* **252**, 1003–1031.

Guckenheimer, J. & Holmes, P. [1993] *Nonlinear Oscillations, Dynamical Systems, and Bifurcations of Vector Fields*, 4th edition (Springer, NY).

Han, M. & Yu, P. [2012] *Normal Forms, Melnikov Functions, and Bifurcations of Limit Cycles* (Springer, NY).

Holling, C. S. [1959a] "The components of predation as revealed by a study of small-mammal predation of the European pine sawfly," *Canad. Entomol.* **91**, 293–320.

Holling, C. S. [1959b] "Some characteristics of simple types of predation and parasitism," *Canad. Entomol.* **91**, 385–398.

Kuznetsov, Yu. A. [1998] *Elements of Applied Bifurcation Theory*, 2nd edition (Springer, NY).

Lotka, A. J. [1920] "Analytical note on certain rhythmic relations in organic systems," *Proc. Natl. Acad. Sci. USA* **6**, 410–415.

Meijer, H., Dercole, F. & Oldemarn, B. [2013] *Numerical Bifurcation Analysis, Encyclopedia of Complexity and Systems Science* (Springer Science + Business Media, NY), pp. 1172–1194.

Rosenzweig, M. L. & MacArthur, R. H. [1963] "Graphical representation and stability conditions of predator–prey interactions," *Amer. Nat.* **97**, 209–223.

Ruan, S. & Wang, W. [2003] "Dynamical behavior of an epidemic model with a nonlinear incidence rate," *J. Diff. Eqs.* **188**, 135–163.

Tian, Y. & Yu, P. [2013] "An explicit recursive formula for computing the normal form and center manifold of n-dimensional differential systems associated with Hopf bifurcation," *Int. J. Bifurcation and Chaos* **23**, 1350104-1–18.

Tian, Y. & Yu, P. [2014] "An explicit recursive formula for computing the normal forms associated with semisimple cases," *Commun. Nonlin. Sci. Numer. Simul.* **19**, 2294–2308.

Volterra, V. [1926] "Variazionie fluttuazioni del numero d'individui in specie animali conviventi," *Mem. Acad. Lincei Roma* **2**, 31–113.

Wang, Y., Wu, H. & Wang, S. [2013] "A predator–prey model characterizing negative effect of prey on its predator," *Appl. Math. Comput.* **219**, 9992–9999.

Xiao, D., Li, W. & Han, M. [2006] "Dynamics in a ratio-dependent predator–prey model with predator harvesting," *J. Math. Anal. Appl.* **324**, 14–29.

Yu, P. [1998] "Computation of normal forms via a perturbation technique," *J. Sound Vib.* **211**, 19–38.

Yu, P. & Leung, A. Y. T. [2003] "The simplest normal form of Hopf bifurcation," *Nonlinearity* **16**, 277–300.

Yu, P. & Han, M. [2005] "Small limit cycles bifurcating from fine focus points in cubic-order Z_2-equivariant vector fields," *Chaos Solit. Fract.* **24**, 329–348.

Yu, P. & Corless, R. M. [2009] "Symbolic computation of limit cycles associated with Hilbert's 16th problem," *Commun. Nonlin. Sci. Numer. Simul.* **14**, 4041–4056.

Yu, P. & Lin, W. [2016] "Complex dynamics in biological systems arising from multiple limit cycle bifurcation," *J. Biol. Dyn.* **10**, 263–285.

Yu, P., Zhang, W. & Wahl, L. M. [2016] "Dynamical analysis and simulation of a 2-dimensional disease model with convex incidence," *Commun. Nonlin. Sci. Numer. Simulat.* **37**, 163–192.

Zhang, W., Wahl, L. M. & Yu, P. [2013] "Conditions for transient viremia in deterministic in-host models: Viral blips need no exogenous trigger," *SIAM J. Appl. Math.* **73**, 853–881.

Zhang, W., Wahl, L. M. & Yu, P. [2014a] "Viral blips may not need a trigger: How transient viremia can arise in deterministic in-host models," *SIAM Rev.* **56**, 127–155.

Zhang, W., Wahl, L. M. & Yu, P. [2014b] "Modelling and analysis of recurrent autoimmune disease," *SIAM J. Appl. Math.* **74**, 1998–2025.